North Carolina State University
Grant NGR-34-002-027 -SC-09447
"Theoretical Investigation of
Liquid Water Injection Into the
Shock Layer of a Reentry Vehicle"
By: Dellinger and Hassan

The Original (Only copy available)

Winnie M. Morgan

GPO PRICE $ _____

CFSTI PRICE(S) $ _____

Hard copy (HC) 3.00

Microfiche (MF) .65

ff 653 July 65

FACILITY FORM 602

N68-18079 (ACCESSION NUMBER)

73 (PAGES)

CR-66562 (NASA CR OR TMX OR AD NUMBER)

1 (THRU)

(CODE)

30 (CATEGORY)

NORTH CAROLINA STATE
OF THE UNIVERSITY OF NORTH CAROLINA
AT RALEIGH

SCHOOL OF ENGINEERING
DEPARTMENT OF MECHANICAL ENGINEERING

NAR-34-002-027

CONTENTS

THEORETICAL INVESTIGATION OF LIQUID WATER INJECTION INTO THE SHOCK LAYER OF A REENTRY VEHICLE

By T. C. Dellinger and H. A. Hassan
North Carolina State University, Raleigh, N. C.

SUMMARY

A method is presented for the calculation of the flow field resulting from the injection of a liquid spray into a supersonic air stream past a blunt body. The model employed assumes a two-phase flow with frozen chemistry and with simultaneous acceleration and evaporation of the spray. The method gives, among other things, the spray penetration. F o r the range of parameters investigated, the penetration increases with an increase in injection speed, angle, and drop size but is almost independent of the mass flow rate. Because the spray acts to slow and to deflect the air stream, there is initially a rise in the air temperature; the magnitude of this rise is such that finite chemical reaction rates should be taken into consideration for more accurate flow field calculations.

INTRODUCTION

The problem of fluid injection into a supersonic stream has been under investigation because of its importance in the areas of communications (e.g. refs. 1,2), aerodynamic control systems (e.g. refs. 3,4) and fuel injection for supersonic combustion (e.g. refs. 5,6). In this work, the injection of liquid water into the supersonic portion of the flow field surrounding a blunt body at typical reentry conditions, with the objective of determining the resulting two-phase flow field and the penetration, is considered. The results of this study have immediate application in the study of material injection as a means of alleviating communications blackout (ref. 7).

Accurate prediction of the fluid penetration is very difficult. The major difficulties being the determination of the shape of the induced shock wave resulting from the obstruction of the primary flow by the emerging jet, and the manner in which a liquid jet breaks up and disperses in the primary flow (ref. 8). For the problem under consideration, it is assumed that the liquid is injected as a uniform spray of spherical drops, and the drop sizes are such that further breakup due to aerodynamic forces is negligible. It is also assumed that the spray is completely porous to the air stream and no shock wave is formed as a result of injection. The first assumption is justified from the consideration that, for the typical reentry conditions considered here, the jet breaks up almost immediately. The second assumption is partially justified if one limits the investigation to dilute sprays. In general, it is believed that the inclusion of a shock wave would only modify rather than alter the results obtained using the shock-free model. This is explained as follows: if a shock forms upstream of the spray, the air stream direction near the body would not be changed greatly from its direction

without a shock; thus, the effects of the relative velocity direction on penetration should not differ very much for the two cases. Also, in the presence of a shock the air velocity seen by the spray is reduced while the air temperature is increased. The reduced air velocity should result in a greater spray penetration in a given distance since the spray is turned in the gas direction at a slower rate; however, the higher air temperature has a counter effect on the penetration since the evaporation is faster and the resulting smaller drops are more quickly entrained by the air stream.

In this work, the analysis treats the air and spray as a two-phase flow problem with simultaneous evaporation and acceleration of the spray, and frozen chemistry. The governing equations are derived in Appendix A using the statistical approach of ref. 9. Because of the type and number of these equations, a numerical solution needs to be employed. The method of integral relations, which was introduced by Dorodnitsyn (ref. 10) is used and the "one-strip" approximation to this method was chosen because past experience, (ref. 11), has shown that it predicts overall flow properties (detachment distance, surface pressure distribution, etc.) fairly well and because it is not as involved as more accurate methods, (ref. 12). It turned out during the course of this investigation that the one-strip approximation was not suited, in its original form, to calculate flow fields, and some modifications were introduced. The numerical calculations were carried out for the NASA RAM C vehicle, which is a slender cone with a spherical nose (fig. 1) for a vehicle speed of 25,920 ft/sec at an altitude of 233,000 ft and zero angle of attack.

ANALYSIS

1. Coordinate System

An orthogonal curvilinear body-oriented coordinate system which is easily adaptable to either two-dimensional or axisymmetric bodies is chosen here. The coordinate system together with pertinent definitions is illustrated in figure 2.

Utilizing the vector operations

$$\phi = \frac{1}{h_s}\frac{\partial \phi}{\partial s}\hat{i}_s + \frac{1}{h_n}\frac{\partial \phi}{\partial n}\hat{i}_n + \frac{1}{h_z}\frac{\partial \phi}{\partial z}\hat{i}_z \tag{1}$$

$$\nabla\cdot\vec{q} = \frac{1}{h_s h_n h_z}\left[\frac{\partial}{\partial s}(q_s h_n h_z) + \frac{\partial}{\partial n}(q_n h_z h_s) + \frac{\partial}{\partial z}(q_z h_s h_n)\right] \tag{2}$$

$$\vec{\nabla}\times\vec{q} = \frac{1}{h_s h_n h_z}\left\{\hat{i}_s\left[\frac{\partial}{\partial n}(h_z q_z) - \frac{\partial}{\partial z}(h_n q_n)\right]\right.$$

$$\left. + \hat{i}_n\left[\frac{\partial}{\partial z}(h_s q_s) - \frac{\partial}{\partial s}(h_z q_z)\right] + \hat{i}_z\left[\frac{\partial}{\partial s}(h_n q_n) - \frac{\partial}{\partial n}(h_s q_s)\right]\right\} \tag{3}$$

and noting that for the orthogonal system under consideration

$$q_z = 0, \quad \frac{\partial}{\partial z} = 0, \quad h_s = 1 + \frac{n}{R}, \quad h_n = 1, \quad h_z = r \tag{4}$$

the dimensionless governing differential equations (38, 39, 41, 42, 43, 44A) take the following forms when $\bar{V}_p = v_s \hat{i}_s + v_n \hat{i}_n$, $\bar{V}_g = u_s \hat{i}_s + u_n \hat{i}_n$:

Spray Continuity

$$\frac{\partial}{\partial s}(r\rho_p v_s) + \frac{\partial}{\partial n}\left[\left(1 + \frac{n}{R}\right) r\rho_p v_n\right] + 3\frac{\beta_1\beta_5\beta_6^2}{\beta_2}\left(1 + \frac{n}{R}\right)\frac{r\rho_p \chi}{r_p^2} = 0 \tag{5}$$

Spray Momentum

$$v_s \frac{\partial v_s}{\partial s} + v_n \frac{\partial}{\partial n}\left[\left(1 + \frac{n}{R}\right) v_s\right] - \frac{3}{8}\frac{\beta_5\beta_6}{\beta_2^2}\left(1 + \frac{n}{R}\right)\frac{\rho_g C_D}{r_p}\left(u_s - \beta_2 v_s\right)\left|\vec{V}_g - \beta_2\vec{V}_p\right| = 0 \tag{6}$$

$$v_s \frac{\partial v_n}{\partial n} - v_s \frac{\partial}{\partial n}\left[\left(1 + \frac{n}{R}\right) v_s\right] + \left(1 + \frac{n}{R}\right)\left(v_s \frac{\partial v_s}{\partial n} + v_n \frac{\partial v_n}{\partial n}\right) - \frac{3}{8}\frac{\beta_5\beta_6}{\beta_2^2}\left(1 + \frac{n}{R}\right)\frac{\rho_g C_D}{r_p}\left(u_n - \beta_2 v_n\right)\left|\vec{V}_g - \beta_2\vec{V}_p\right| = 0 \tag{7}$$

Droplet Radius

$$v_s \frac{\partial r_p}{\partial s} + \left(1 + \frac{n}{R}\right) v_n \frac{\partial r_p}{\partial n} + \frac{\beta_1\beta_5\beta_6^2}{\beta_2}\left(1 + \frac{n}{R}\right)\frac{\chi}{r_p} = 0 \tag{8}$$

Gas Continuity

$$\frac{\partial}{\partial s}(r\rho_g u_s) + \frac{\partial}{\partial n}\left[\left(1 + \frac{n}{R}\right) r\rho_g u_n\right] - 3\beta_1\beta_3\beta_5\beta_6^2\left(1 + \frac{n}{R}\right)\frac{r\rho_p \chi}{r_p^2} = 0 \tag{9}$$

Gas Momentum

$$u_s \frac{\partial u_s}{\partial s} + \frac{\beta_4}{\rho_g} \frac{\partial p}{\partial s} + u_n \frac{\partial}{\partial n} [(1 + \frac{n}{R}) u_s]$$

$$+ 3\beta_3\beta_5\beta_6 (1 + \frac{n}{R}) \frac{\rho_p}{\rho_g r_p} (u_s - \beta_2 v_s) [\frac{\rho_g C_D}{8} |\vec{V}_g - \beta_2 \vec{V}_p|$$

$$+ \beta_1\beta_6 \frac{\chi}{r_p}] = 0 \qquad (10)$$

$$u_s \frac{\partial u_n}{\partial s} - u_s \frac{\partial}{\partial n} [(1 + \frac{n}{R}) u_s] + (1 + \frac{n}{R}) [\frac{\beta_4}{\rho_g} \frac{\partial p}{\partial n} + u_s \frac{\partial u_s}{\partial n} + u_n \frac{\partial u_n}{\partial n}]$$

$$+ 3\beta_3\beta_5\beta_6 (1 + \frac{n}{R}) \frac{\rho_p}{\rho_g r_p} (u_n - \beta_2 v_n) [\frac{\rho_g C_D}{8} |\vec{V}_g - \beta_2 \vec{V}_p|$$

$$+ \beta_1\beta_6 \frac{\chi}{r_p}] = 0 \qquad (11)$$

Gas Energy

$$\frac{\partial}{\partial s} [r\rho_g u_s (h_g + \frac{u_s^2+u_n^2}{2})] + \frac{\partial}{\partial n} [(1 + \frac{n}{R}) r\rho_g u_n (h_g + \frac{u_s^2+u_n^2}{2})]$$

$$+ 3\beta_2\beta_3\beta_5\beta_6 (1 + \frac{n}{R}) \frac{r\rho_p}{r_p} [\frac{\rho_g C_D}{8} |\bar{V}_g - \beta_2 \bar{V}_p| (\vec{V}_g - \beta_2 \vec{V}_p) \cdot \vec{V}_p$$

$$- \beta_1\beta_2\beta_6 \frac{\chi}{r_p} (h_p + \frac{v_s^2 + v_n^2}{2})] = 0 \qquad (12)$$

2. Divergence Form of the Governing Equations

Application of the integral method requires that the governing equations be put into the divergence form,

$$\frac{\partial I_i}{\partial s} + \frac{\partial G_i}{\partial n} + K_i = 0 \quad . \qquad (13)$$

As seen above, some of the equations, namely (5), (9) and (12), are already in this form. There are, however, many ways in which these equations and the remaining equations can be put in divergence form, and the solution will depend on the particular form chosen when a finite number of strips is

employed, (ref. 13). The particular expressions chosen for the I_i, G_i and K_i functions are given below.

Spray Continuity

$$i = 1,\ I_1 = r\rho_p v_s,\ G_1 = \left(1 + \frac{n}{R}\right) r\rho_p v_n,\ K_1 = 3\,\frac{\beta_1\beta_5\beta_6^2}{\beta_2}\left(1 + \frac{n}{R}\right)\frac{r\rho_p \chi}{r_p^2} \tag{14}$$

Gas Continuity

$$i = 2,\ I_2 = r\rho_g u_s,\ G_2 = \left(1 + \frac{n}{R}\right) r\rho_g u_n,\ K_2 = -3\beta_1\beta_3\beta_5\beta_6^2\left(1 + \frac{n}{R}\right)\frac{r\rho_p \chi}{r_p^2} \tag{15}$$

Droplet Radius

$$i = 3,\ I_3 = r\rho_p v_s r_p,\ G_3 = r\rho_p v_n r_p,\ K_3 = 4\,\frac{\beta_1\beta_5\beta_6^2}{\beta_2}\left(1 + \frac{n}{R}\right)\frac{r\rho_p \chi}{r_p} \tag{16}$$

Spray Momentum

$$i = 4,\ I_4 = r\rho_p v_s^2,\quad G_4 = \left(1 + \frac{n}{R}\right) r\rho_p v_s v_n$$

$$K_4 = \frac{r\rho_p v_s v_n}{R} - 3\,\frac{\beta_5\beta_6}{\beta_2^2}\left(1 + \frac{n}{R}\right)\frac{r\rho_p}{r_p}\left[\frac{\rho_g C_D}{8}\left(u_s - \beta_2 v_s\right)\left|\vec{V}_g - \beta_2\vec{V}_p\right|\right.$$

$$\left. - \beta_1\beta_2\beta_6\,\frac{\chi v_s}{r_p}\right] \tag{17}$$

$$i = 5,\ I_5 = r\rho_p v_s v_n,\quad G_5 = \left(1 + \frac{n}{R}\right) r\rho_p v_n^2$$

$$K_5 = -\frac{r\rho_p v_s^2}{R} - 3\,\frac{\beta_5\beta_6}{\beta_2^2}\left(1 + \frac{n}{R}\right)\frac{r\rho_p}{r_p}\left[\frac{\rho_g C_D}{8}\left(u_n - \beta_2 v_n\right)\left|\vec{V}_g - \beta_2\vec{V}_p\right|\right.$$

$$\left. - \beta_1\beta_2\beta_6\,\frac{\chi v_n}{r_p}\right] \tag{18}$$

Gas Momentum

$$i = 6, \quad I_6 = r(\rho_g u_s^2 + \beta_4 p_g), \quad G_6 = \left(1 + \frac{n}{R}\right) r\rho_g u_s u_n$$

$$K_6 = \frac{r\rho_g u_s u_n}{R} - \beta_4 p_g \sin\theta + 3\beta_3\beta_5\beta_6 \left(1 + \frac{n}{R}\right) \frac{r\rho_p}{r_p}$$

$$\cdot \left[\frac{\rho_g C_D}{8} (u_s - \beta_2 v_s)\left|\vec{V}_g - \beta_2\vec{V}_p\right| - \beta_1\beta_2\beta_6 \frac{\chi v_s}{r_p}\right] \qquad (19)$$

$$i = 7, \quad I_7 = r\rho_g u_s u_n, \quad G_7 = \left(1 + \frac{n}{R}\right) r(\rho_g u_n^2 + \beta_4 p_g)$$

$$K_7 = -\frac{r\rho_g u_s^2}{R} - \beta_4 p_g \left[\frac{r}{R} + \left(1 + \frac{n}{R}\right)\cos\theta\right] + 3\beta_3\beta_5\beta_6 \left(1 + \frac{n}{R}\right) \frac{r\rho_p}{r_p}$$

$$\cdot \left[\frac{\rho_g C_D}{8} (u_n - \beta_2 v_n)\left|\vec{V}_g - \beta_2\vec{V}_p\right| - \beta_1\beta_2\beta_6 \frac{\chi v_n}{r_p}\right] \qquad (20)$$

Gas Energy

$$i = 8, \quad I_8 = r\rho_g u_s \left(h_g + \frac{u_s^2 + u_n^2}{2}\right), \quad G_8 = \left(1 + \frac{n}{R}\right) r\rho_g u_n \left(h_g + \frac{u_s^2 + u_n^2}{2}\right)$$

$$K_8 = 3\beta_2\beta_3\beta_5\beta_6 \left(1 + \frac{n}{R}\right) \frac{r\rho_p}{r_p} \cdot \left\{\frac{\rho_g C_D}{8}\left|\vec{V}_g - \beta_2\vec{V}_p\right| [v_s(u_s - \beta_2 v_s)\right.$$

$$\left. + v_n(u_n - \beta_2 v_n)\right] - \beta_1\beta_2\beta_6 \frac{\chi}{r_p} \left(h_p + \frac{v_s^2 + v_n^2}{2}\right)\} \qquad (21)$$

3. Integral Form of the Equations

In order to utilize the method of integral relations, a choice must be made for the number of strips to be used. The simplest choice is one strip with the I_i terms being approximated by functions linear in n. Although this approximation might seem rather crude, actual calculations using this approach are sufficiently accurate when only information along the strip boundaries is desired, (ref. 11); however, results predicted using this procedure are somewhat approximate, at intermediate points (ref. 13). Because the total number of equations is more than doubled when injection is considered, the actual number of equations required for the calculations can become quite large when multi-strip schemes are employed. Therefore, a

modified one-strip method which allows for more accurate flow field calculations is employed.

A schematic of the flow field to be analyzed here is shown in figure 3. The interface ϵ determines the penetration of the spray. The interface represents a discontinuity in the spray density because $\lim_{n\to\epsilon^+} \rho_p = 0$ and $\lim_{n\to\epsilon^-} \rho_p \neq 0$; however, the interface is assumed completely porous to the gas flow. Between the interface and the body ($0 \leq n \leq \epsilon$), the spray equations (14), (16), (17), (18) and the gas equations (15), (19), (20) and (21) need to be considered while in the region between the shock wave and interface ($\epsilon \leq n \leq \delta$) only the gas equations (15), (19) and (20) need to be considered. Using the given flow field model and integrating equations (14), (16), (17), (18), and (21) between 0 and ϵ and equations (15), (19) and (20) between 0 and δ and utilizing Leibnitz's rule, one finds

$$\frac{d}{ds}\int_0^{\epsilon} I_i dn = I_{i\epsilon}\frac{d\epsilon}{ds} + G_{io} - G_{i\epsilon} - \int_0^{\epsilon} K_i dn, \quad i = 1,3,4,5,8 \tag{22}$$

$$\frac{d}{ds}\int_0^{\delta} I_j dn = I_{j\delta}\frac{d\delta}{ds} + G_{jo} - G_{j\delta} - \int_0^{\delta} K_j dn, \quad j = 2,6,7 \tag{23}$$

where the subscripts 0, ϵ and δ represent the body, interface and shock, respectively. Equations (22) and (23) contain the undefined quantities $d\epsilon/ds$ and $d\delta/ds$, respectively. From the geometry of the shock wave one has, (ref. 12)

$$d\delta/ds = (1 + \delta/R)\cot(\nu + \theta) . \tag{24}$$

Since the spray does not penetrate the interface, it must be a streamline for the spray; hence,

$$d\epsilon/ds = v_{n\epsilon}/v_{s\epsilon} = I_{5\epsilon}/I_{4\epsilon} . \tag{25}$$

Since K_j, $j = 2,6,7$ is discontinuous, equation (23) requires further consideration. As was pointed out above, Leibnitz's rule is used to reduce the integrals $\int_0^{\delta} (\partial I_j/\partial s)dn$, $j = 2,6,7$. This step requires that I_j and $\partial I_j/\partial s$ be continuous within $0 \leq n \leq \delta$; hence, continuity of all gas properties at the interface is assumed. From a consideration of the general divergence form of the governing equation, one can reason that the discontinuity in $K_{j\epsilon}$ should be reflected in the $(\partial G_j/\partial n)_\epsilon$ terms since the $(\partial I_j/\partial s)_\epsilon$ terms are assumed continuous as required by Leibnitz's rule. For this reason, when representing I_i as $I_i(s,n)$, the normal derivatives of the gas properties at ϵ are assumed to be discontinuous. It should be noted, however, that, within

the framework of the method of integral relations, one needs not invoke such an assumption. This follows because the governing equations are equations (22) and (23) rather than the divergence form equations, and equation (23) is valid even when the integrand $(\partial G_j/\partial n)$ is discontinuous at a finite number of points between $0 \leq n \leq \delta$. The assumption of discontinuous derivatives for the gas properties at ϵ is employed here because it is believed to be more representative of the actual situation.

4. Flux Approximations

As can be seen from the divergence form of the governing equations, the quantities I_i $(i = 1,3,4,5,8)$ and I_j $(j = 2,6,7)$ are products of the spray and gas properties, respectively. These products, which we will hereafter refer to as the fluxes, appear as integrands in the integral relations (22) and (23). In order to evaluate these integrals, the n-variation of the fluxes must be specified. In the one-strip approximation, it is usually assumed that the fluxes vary linearly between the strip boundaries (ref. 12). In this work, such an assumption is relaxed and the various fluxes are approximated as follows.

For the range $0 \leq n \leq \epsilon$, we assume that

$$I_i = I_{io} + (I_{i\epsilon} - I_{io}) f_i(w), \quad w = n/\epsilon$$
$$f_i(0) = 0, \quad f_i(1) = 1, \quad i = 1,3,4,5,8 \tag{26}$$

where $f_i(w)$ is some polynomial, not necessarily linear. For $0 \leq n \leq \delta$, we seek approximations of the form

$$I_j = I_{jo} + (I_{j\delta} - I_{jo}) f_j(z), \quad z = n/\delta$$
$$f_j(0) = 0, \quad f_j(1) = 1, \quad j = 2,6,7 \ . \tag{27}$$

However, the normal derivatives of the gas properties at ϵ are postulated as being discontinuous so that the expressions (27) are replaced,

for $\frac{\epsilon}{\delta} \leq z \leq 1$, by

$$I_j = I_{jo} + (I_{j\delta} - I_{jo})\ {}_{\delta}f_j(z)$$
$${}_{\delta}f_j(1) = 1, \quad j = 2,6,7 \tag{28}$$

and for $0 \leq z \leq \epsilon/\delta$, by

$$I_j = I_{jo} + (I_{j\delta} - I_{jo})\ {}_{\epsilon}f_j(z)$$
$${}_{\epsilon}f_j(0) = 0, \quad {}_{\epsilon}f_j(\epsilon/\delta) = {}_{\delta}f_j(\epsilon/\delta), \quad j = 2,6,7 \ . \tag{29}$$

The condition on ${}_{\epsilon}f(\epsilon/\delta)$ given in (29) follows from the fact that

I_j ($j = 2,6,7$) is assumed continuous at ϵ. Here, also, ${}_{\epsilon}f_j(z)$ and ${}_{\delta}f_j(z)$ are polynomials, not necessarily linear.

Using the preceding approximations (26), (28) and (29), the integrals of the fluxes in equations (22) and (23) can be evaluated, giving

$$\frac{d}{ds}\{\epsilon[I_{io} + (I_{i\epsilon}-I_{io})q_i]\} = I_{i\epsilon}\frac{d\epsilon}{ds} + G_{io} - G_{i\epsilon} - \epsilon\int_0^1 K_i dw$$

$$q_i = \int_0^1 f_i(w)dw, \quad i = 1,3,4,5,8 \tag{30}$$

and

$$\frac{d}{ds}\{\delta[I_{jo} + (I_{j\delta}-I_{jo})q_j]\} = I_{j\delta}\frac{d\delta}{ds} + G_{jo} - G_{j\delta} - \delta\int_0^1 K_j dz$$

$$q_j = \int_0^1 f_j(z)dz = \int_0^{\epsilon/\delta} {}_{\epsilon}f_j(z)dz + \int_{\epsilon/\delta}^1 {}_{\delta}f_j(z)dz, \quad j = 2,6,7 \tag{31}$$

For equation (30) we define the general dependent variable, ξ_i, given by

$$\xi_i = \epsilon[I_{io} + (I_{i\epsilon}-I_{io})q_i], \quad i = 1,3,4,5,8 \tag{32}$$

so that equation (30) becomes

$$\frac{d\xi_i}{ds} = I_{i\epsilon}\frac{d\epsilon}{ds} + G_{io} - G_{i\epsilon} - \epsilon\int_0^1 K_i dw, \quad i = 1,3,4,5,8\ . \tag{33}$$

For equations $j = 2,6$ of equation (31), we define the dependent variable

$$\xi_j = I_{jo} + (I_{j\delta}-I_{jo})q_j, \quad j = 2,6 \tag{34}$$

where

$$\frac{d\xi_j}{ds} = \frac{1}{\delta}\left[(I_{j\delta}-\xi_j)\frac{d\delta}{ds} + G_{jo} - G_{j\delta}\right] - \int_0^1 K_j dz, \quad j = 2,6\ . \tag{35}$$

Equation $j = 7$ is a special case of equations (34) and (35) above in which $I_{70} = 0$ because $u_{no} = 0$. It will be assumed that q_7 = constant and for $j = 7$ we define

$$\xi_7 = I_{7\delta} \tag{36}$$

and we obtain

$$\frac{d\xi_7}{ds} = \frac{1}{\delta q_7}\left[(1-q_7)\,\xi_7\,\frac{d\delta}{ds} + G_{70} - G_{78}\right] - \frac{1}{q_7}\int_0^1 K_7 dz \quad . \tag{37}$$

The assumption that q_7 = constant is discussed in the section on boundary conditions.

The above expressions (33), (35) and (37) are a set of ordinary differential equations which may be integrated numerically for given initial and boundary conditions. Such conditions are discussed in the following sections.

5. Modifications of the One-Strip Approximation

In the preceding sections, the one-strip approximation was applied to the governing gas and spray equations. As a result, an approximate set of governing differential equations was obtained. The dependent variables ξ are given in terms of the flux values on the strip boundaries and the integrals of the assumed distributions between the strip boundaries. When one strip is used, the usual procedure is to assume that the distributions are linear and to impose boundary conditions on the properties along one of the two boundaries. The ordinary differential equation solutions can then be used to determine the unknown properties along the remaining boundary. Such boundary properties are generally accurate, but the flow field values are usually not accurate. In theory, this problem can be overcome by increasing the number of strips. However, if the one-strip formulation is to be used and more accurate flow-field properties are desired, an alternative approach to the usual one-strip integral method must be used.

One possible procedure is not to assume linear distributions and to obtain additional conditions which will allow one to adjust the distributions f (or q) as the calculation proceeds. Additional conditions at the boundaries can be obtained by utilizing the exact governing differential equations; that is, by taking the limit of equation (13) as n approaches 0 or ϵ. Conditions generated by this procedure result in total differential equations which, when combined with equations (30) and (31), give sufficient information to change f or q.

BOUNDARY CONDITIONS

1. Gas

Since the gas dependent variables are given by the equations [(32), j = 8], [(34), j = 2,6] and [(36), j = 7], values for the fluxes I_j (j = 2,6, 7,8) are desired along the shock, interface and body.

a. Shock

The desired shock conditions are those corresponding to the passage of a thermally perfect, calorically imperfect gas of constant chemical composition through a locally straight oblique shock wave. For given free stream conditions and either one property behind the shock or the shock wave angle, ν, the remaining properties behind the shock can be determined from the Rankine-Hugoniot equations. As shown in the derivative of equation (37), using $u_{no} = 0$ and assuming q_7 constant leads to a differential equation for $I_{7\delta}$. This equation, when coupled with the Rankine-Hugoniot equations and equation (24), leads to two non-linear algebraic equations for ν and $T_{g\delta}$. These two equations can be solved simultaneously by an iterative procedure. Once values of ν and $T_{g\delta}$ are known, the remaining shock properties can be calculated.

b. Interface

Continuity of all gas properties is required at the interface, but the normal derivatives of these properties are assumed discontinuous. In addition, a condition on $I_{8\epsilon}$ is obtained since $I_{8\epsilon} = I_{2\epsilon}H$, where H is the total enthalpy of the gas and is constant for $n \geq \epsilon$.

c. Body

The boundary condition $u_{no} = 0$ gives I_{7o}, a result which has been used in deriving equation (39). In order to obtain values for the gas properties I_{jo} $(j = 2,6,8)$, we consider the exact equation for the properties, i.e., $(\partial I_j/\partial s) + (\partial G_j/\partial n) + K_j = 0$. Taking the limit as $n \to 0$ and utilizing equations [(26), $j = 8$] and [(29), $j = 2,6$] gives

$$\frac{dI_{jo}}{ds} + \lim_{n\to 0} \left(\frac{\partial G_j}{\partial n}\right) + K_{jo} = 0, \quad j = 2,6,8 . \tag{38}$$

However, $G_j = \left(1 + \frac{n}{R}\right) I_j \frac{u_n}{u_s}$, so that

$$\lim_{\substack{n\to 0 \\ u_n \to 0}} \left(\frac{\partial G_j}{\partial n}\right) = \frac{I_{jo}}{u_{so}} \left(\frac{\partial u_n}{\partial n}\right)_0 , \quad j = 2,6,8 . \tag{39}$$

Since $u_n = I_7/I_2$, we have

$$\left(\frac{\partial u_n}{\partial n}\right)_0 = \frac{1}{I_{20}} \left(\frac{\partial I_7}{\partial n}\right)_0 . \tag{40}$$

Thus, we obtain the following condition which must be satisfied by the gas properties at the body:

$$\frac{dI_{jo}}{ds} = -K_{jo} - \frac{I_{jo}}{u_{so} I_{20}} \left(\frac{\partial I_7}{\partial n}\right)_0 , \qquad j = 2,6,8 . \tag{41}$$

Values for $(\partial I_7/\partial n)_0 = \xi_7 (\partial f_7/\partial n)_0$ are dependent upon the polynomial approximation chosen for f_7.

d. Polynomial Approximations

Simultaneous solution of the differential equations (35), (37) and (41) yields values for I_{jo} $(j = 2,6,8)$, $I_{j\delta}$ $(j = 2,6,7)$ and ξ_j $(j = 2,6)$. From these one can calculate the values for q_2 and q_6 since

$$q_j = \frac{\xi_j - I_{jo}}{I_{j\delta} - I_{jo}} , \qquad j = 2,6 . \tag{42}$$

The question arises as how to select f_2, f_6 and f_7 so as to satisfy equation (42) for q_2, q_6 and the assumed value of q_7. Since the solution of the general problem is started at a point where the distribution of the gas properties in the shock layer is assumed known, the distributions f_2, f_6 and f_7 and the corresponding integrals q_2, q_6 and q_7 are completely determined initially. A close approximation to the initial data (ref. 14) was obtained by assuming the following polynomial approximations:

$$f_j(z) = z[a_{1j}(z^4-1) + a_{2j}(z^3-1) + a_{3j}(z^2-1) + a_{4j}(z-1) + 1], \quad j = 2,6 \tag{43}$$

and

$$f_7(z) = z^3 \left(\frac{I_2}{I_{2\delta}}\right)_{\text{initial}} \equiv z^3[a_{17}(z-1) + a_{27}(z^2-1) + a_{37}(z^3-1) + a_{47}(z^4-1) + a_{57}(z^5-1) + 1] . \tag{44}$$

The coefficients a_{ij} are known constants, and the expression for f_7 results from taking $u_n = z^3 u_{n\delta}$, $z = n/\delta$.

Downstream of the initial line, the distributions are as follows: Due to the postulated discontinuity in the slopes of the gas properties at the interface, we take

$$f_j(z) = {}_{\delta}f_j(z) \ , \quad \epsilon/\delta \leq z \leq 1$$
$$f_j(z) = {}_{\epsilon}f_j(z) \ , \quad 0 \leq z \leq \epsilon/\delta \qquad j = 2,6,7 \tag{45}$$

where ${}_{\delta}f_j(\epsilon/\delta) = {}_{\epsilon}f_j(\epsilon/\delta)$. For the region $\epsilon/\delta \leq z \leq 1$, the form of the distributions ${}_{\delta}f_j$ $(j = 2,6,7)$ is taken to be the form used for the initial line distributions, equations (43) and (44). For the region $0 \leq z \leq \epsilon/\delta$, we assume that the distributions are linear in z, so that

$${}_{\epsilon}f_j(z) = {}_{\delta}f_j(\epsilon/\delta)[z/(\epsilon/\delta)] \qquad j = 2,6,7 \ . \tag{46}$$

Recalling that q_j is defined as $q_j = \int_0^1 f_j(z)dz$, one finds

$$q_j = \int_0^{\epsilon/\delta} {}_{\epsilon}f_j(z)dz + \int_{\epsilon/\delta}^{1} {}_{\delta}f_j(z)dz = (\epsilon/2\delta)\ {}_{\delta}f_j(\epsilon/\delta) + \int_{\epsilon/\delta}^{1} {}_{\delta}f_j(z)dz \ . \tag{47}$$

Thus, equation (47) represents the relation which the coefficients a_{ij} must satisfy so that the resulting q_j's coincide with values obtained from equation (42) and q_7, which is assumed constant at its initial value. Since there is no unique way of selecting these coefficients, it was assumed that for each j, $(j = 2,6,7)$, all but one of the coefficients a_{ij} remained constant. The variable coefficient was determined from equation (47) by utilizing equation (42) and the known value of q_7.

Because the distributions ${}_{\epsilon}f_2$, ${}_{\epsilon}f_6$ and ${}_{\epsilon}f_7$ were taken as linear functions a similar variation was assumed for f_8, i.e.,

$$f_8(w) = w = z/(\epsilon/\delta) \ . \tag{48}$$

Values for I_{80} are calculated from equation (41) and the flux values at the interface are given by $I_{8\epsilon} = I_{2\epsilon}$ H. Introducing the linear approximation of equation (48) means that the gas energy f l u x is completely determined in the region $0 \leq n \leq \epsilon$, since

$$I_8 = I_{80} + (I_{8\epsilon} - I_{80})\ f_8\ (w) \ .$$

As is seen from the above, I_8 is calculated without using equation (33) for $j = 8$. This suggests that one can choose $f_8(w)$ as a higher degree polynomial and utilize equation (33) to change the distribution. This procedure was

employed first but was later abandoned because it resulted in numerical instabilities.

The above gas model is a so-called "hybrid" because both equations (33) and (41) are employed in calculating the flow properties.

2. Spray

The spray dependent variables are governed by equations [(32), i = 1,3, 4,5], and values for the fluxes I_i (i = 1,3,4,5) are desired along the body and the interface.

The boundary conditions depend upon the manner in which the spray is injected. In this work, it was desired to investigate the case of discrete injection; that is, injection over a finite distance along the body followed by a region in which no injection occurs. The following injection model was used:

First, a uniform injection region occurs in which the spray is injected at assigned constant properties which are independent of body location. This region is followed by a narrow transition region in which the normal component of the velocity is decreased to zero while keeping the magnitude of the velocity and the other injection properties constant. A value of zero for the normal component of the spray velocity at the body characterizes the condition of no injection.

In the preceding model, the meaning of the last region is obvious; however, the other two regions deserve comment. In the uniform injection region, the choice of constant properties was made for reasons of convenience only, and the method presented in the following sections can be applied to any other choice of injection parameters. The transition region serves the purpose of turning the injected spray during the final stages of injection so that the spray flows parallel to the body when injection ceases. The reasons for including a transition injection region are as follows: As is shown in figure 4, it is suspected that when an injection region is immediately followed by a region of no injection, the spray separates from the wall but reattaches a short distance downstream. After reattachment, the spray at the body is characterized by the condition that the normal component of the velocity is zero; i.e., $v_{no} = 0$. Because the gas and spray equations developed in this work do not account for any viscous effects, an injection model was chosen that included a region in which the spray injection angle could be turned in a continuous manner from its uniform injection value to a value parallel to the body some distance downstream.

Boundary conditions on the spray properties are given below for the uniform injection ($s_o \leq s \leq s_1$); transition ($s_1 \leq s \leq s_2$); and no injection ($s \geq s_2$) regions.

a. Uniform Injection Region

For this region, the flux values at the body are assumed given, and the spray properties (ρ_p, r_p, V_p) are assumed independent of body location. Since the properties at injection are used as normalizing factors, the injection process is characterized by the dimensionless variables

$$\rho_{po} = v_{no} = r_{po} = 1 . \tag{49}$$

The angle of injection ϕ with respect to the body is also constant and is defined by

$$\frac{v_{no}}{v_{so}} = \tan \phi \tag{50}$$

so that

$$v_{so} = \cot \phi = \text{constant} . \tag{51}$$

From the above it follows that the flux variations along the body for the spray are given by

$$\frac{dI_{io}}{ds} = \frac{I_{io}}{r_o} \sin \theta , \quad i = 1,3,4,5 \tag{52}$$

where I_{io}/r_o = constant and $\sin \theta = dr_o/ds$ = constant, the latter condition results from the fact that the body radius of curvature is infinite throughout the region $s \geq s_o$ for the RAM C vehicle considered in this work.

The boundary conditions, equations (52), when combined with the limiting form of the governing equations lead to some conditions that must be satisfied by the distribution functions f_i. Thus, the limit as $n \to 0$ of equation (13) yields

$$\frac{dI_{io}}{ds} + \lim_{n \to 0} \left(\frac{\partial G_i}{\partial n}\right) + K_{io} = 0 , \quad i = 1,3,4,5 . \tag{53}$$

Using $G_i = I_i I_5 / I_4$ and equations (26), (32) and (52) in the above equation, the following result is obtained:

$$\frac{1}{q_i}\left(\frac{\partial f_i}{\partial w}\right)_0 = \frac{f'_{io}}{q_i} = I_{io} \frac{I_{40}}{I_{50}} \left(\frac{\epsilon}{\frac{\xi_i}{\epsilon} - I_{io}}\right)\left(\frac{K_{50}}{I_{50}} - \frac{K_{40}}{I_{40}} - \frac{K_{io}}{I_{io}} - \frac{\sin \theta}{r_o}\right) \tag{54}$$

$$i = 1,3,4,5 .$$

The above condition on $f_i(w)$ represents a third condition to be used with the two conditions of equation (26); i.e., $f_i(0) = 0$ and $f_i(1) = 1$. These

three conditions make it possible to choose second order polynomials for the functions $f_i(w)$, $i = 1,3,4,5$ as follows:

When $f'_{io} \leq 1$, we take

$$f_i(w) = a_i w + (1-a_i)\, w^2 \tag{55}$$

where

$$a_i = 2 \,/\, \left(\frac{6q_i}{f'_{io}} - 1\right) \tag{56}$$

and whenever $f'_{io} > 1$, we take

$$f_i(w) = \frac{1}{2}\left[-b_i + \sqrt{b_i^2 + 4(1 + b_i)\, w}\,\right] \tag{57}$$

where

$$b_i = \frac{1}{2}\left[-B + \sqrt{B^2 - 4AC}\,\right], \quad b_i > 0$$

$$A = 1, \quad B = \frac{4\,\frac{f'_{io}}{q_i} - 12}{3\,\frac{f'_{io}}{q_i} - 6}, \quad C = \frac{2}{2 - \frac{f'_{io}}{q_i}} \tag{58}$$

Expression (57) has the property that $q_i \longrightarrow 2/3$ as $f'_{io} \longrightarrow \infty$.

b. Transition Region

This region is intended as a region of transition between the uniform injection region where $v_{no} = 1$ and the no-injection region characterized by $v_{no} = 0$. In this region it is assumed that

$$\rho_{po} = r_{po} = 1, \quad V_{po} = \text{constant} \tag{59}$$

and

$$v_{no} = 1 - 3\left(\frac{s-s_1}{s_2-s_1}\right)^2 + 2\left(\frac{s-s_1}{s_2-s_1}\right)^3 \tag{60}$$

where v_{no} satisfies the following conditions:

$$s = s_1: \quad v_{no} = 1, \quad dv_{no}/ds = 0$$
$$s = s_2: \quad v_{no} = 0, \quad dv_{no}/ds = 0 \,. \tag{61}$$

Since the injection is assumed to occur at the constant velocity of the uniform injection region, the tangential injection velocity is given by

$$v_{so}^2 = V_{po}^2 - v_{no}^2 \,. \tag{62}$$

The flux variations along the body are then given by

$$\frac{dI_{10}}{ds} = \frac{dI_{30}}{ds} = r_o \frac{dv_{so}}{ds} + v_{so} \sin\theta$$
$$\frac{dI_{40}}{ds} = I_{10} \frac{dv_{so}}{ds} + v_{so} \frac{dI_{10}}{ds} \tag{63}$$
$$\frac{dI_{50}}{ds} = I_{10} \frac{dv_{no}}{ds} + v_{no} \frac{dI_{10}}{ds}$$

where $\dfrac{dv_{so}}{ds} = -\dfrac{v_{no}}{v_{so}} \dfrac{dv_{no}}{ds}$. In the uniform injection region, equations (52) and (53) were combined to obtain conditions on the flux distributions of the spray, f_i. Here, the set of equations (63) corresponds to the set (52), which seems to indicate that a similar procedure for obtaining conditions on the f_i could be followed for this region as for the uniform injection region. However, the $i = 5$ equation of the set (53) is satisfied identically when $v_{no} \longrightarrow 0$ so that the conditions obtained for the f_i are singular at that point.

Instead, we consider equation (13) as before, but take the limit as $n \longrightarrow \epsilon$, which leads to

$$\frac{dI_{i\epsilon}}{ds} - \left(\frac{I_{i\epsilon} - I_{io}}{\epsilon}\right) \frac{d\epsilon}{ds} f'_{i\epsilon} + \lim_{n \to \epsilon} \left(\frac{\partial G_i}{\partial n}\right) + K_{i\epsilon} = 0 \,, \quad i = 1,3,4,5 \tag{64}$$

where the above result is obtained using $I_i = I_{io} + (I_{i\epsilon} - I_{io}) f_i$. Using equation (32), the following expression for $dI_{i\epsilon}/ds$ results:

$$\frac{dI_{i\epsilon}}{ds} = \frac{1}{q_i} \left[\frac{d}{ds}\left(\frac{\xi_i}{\epsilon}\right) - (1-q_i) \frac{dI_{io}}{ds}\right] - \frac{1}{2 q_i} \left(\frac{\xi_i}{\epsilon} - I_{io}\right) \frac{dq_i}{ds} \,, \quad i = 1,3,4,5 \,. \tag{65}$$

Substituting in (64) for $dI_{i\epsilon}/ds$ and recalling that $G_i = I_i I_5/I_4$ gives

$$\frac{(\frac{\xi_i}{\epsilon} - I_{io})}{q_i}\frac{dq_i}{ds} = \frac{d}{ds}(\frac{\xi_i}{\epsilon}) - (1-q_i)\frac{dI_{io}}{ds} + q_i K_{i\epsilon}$$
$$+ \frac{q_i I_{i\epsilon}}{\epsilon\, I_{4\epsilon}}\left[(\frac{\xi_5}{\epsilon} - I_{50})\frac{f'_{5\epsilon}}{q_5} - (\frac{\xi_4}{\epsilon} - I_{40})\frac{d\epsilon}{ds}\frac{f'_{4\epsilon}}{q_4}\right], \quad i = 1,3,4,5 . \tag{66}$$

Since the derivatives $d\epsilon/ds$, $d\xi_i/ds$ and dI_{io}/ds can be calculated from equations (25), (33) and (63) respectively, equation (66) can be used to calculate q_i and provides the desired condition on f_i in the transition region. The distributions (55) and (57) are again used, but the coefficients are now given by

$$a_i = 6q_i - 2 \quad \text{and} \quad b_i = \frac{4-6q_i}{6q_i-3} . \tag{67}$$

c. No-injection Region

This region is characterized by $v_{no} = 0$ throughout. This condition alone does not give enough information to determine the flow field completely. Additional boundary conditions can be obtained by using the limiting form of the equations at 0 and ϵ. When these equations are used in conjunction with equation (30), one can calculate the fluxes at both boundaries and the changes in the distribution functions. However, based on the numerical results obtained by such a procedure, it was concluded that such a combination of equations is not compatible.

To proceed further one has two choices: to assume enough values at the boundaries so that the schemes used in the injection region can be employed, or to assume q_i = constant. Since properties at the body are part of the desired information, the latter assumption is used. In this case, one can use equations (53) and (64) or equations (53) and (30). The first set of equations is more convenient and is employed.

In the no-injection region, equation (53) becomes

$$\frac{dI_{io}}{ds} + \frac{I_{io}}{I_{40}}\left(\frac{\partial I_5}{\partial n}\right)_0 + K_{io} = 0 , \quad i = 1,3,4 . \tag{68}$$

Due to the influence of the I_5 distribution, it was felt that the assumption q_5 = constant was highly restrictive. A procedure whereby such an assumption

can be relaxed is obtained from the following consideration. Since the injection in the preceding transition region turns the spray parallel to the body, it is assumed that in the no-injection region the spray and gas rapidly adjust to the condition

$$\lim_{\bar{n}\to 0} \left(\frac{\partial \bar{v}_n}{\partial \bar{n}}\right) = \lim_{\bar{n}\to 0} \left(\frac{\partial \bar{u}_n}{\partial \bar{n}}\right) \tag{69}$$

where the superscript bars denote dimensional variables. The dimensionless form of (69) is

$$\left(\frac{\partial v_n}{\partial n}\right)_0 = \frac{1}{\beta_2} \left(\frac{\partial u_n}{\partial n}\right)_0 . \tag{70}$$

As an approximation, this condition is imposed at the very beginning of the no-injection region. Thus, since

$$\left(\frac{\partial v_n}{\partial n}\right)_0 = \frac{I_{5\epsilon} f'_{50}}{I_{10^\epsilon}} \tag{71}$$

it follows that the expression

$$f'_{50} = \frac{\epsilon\, I_{10}}{\beta_2 I_{5\epsilon}} \left(\frac{\partial u_n}{\partial n}\right)_0 \tag{72}$$

when combined with the conditions $f_5(0) = 0$ and $f_5(1) = 1$ can be used to determine the f_5 distribution throughout the no-injection region. As before, either equation (55) or (57) determines f_5.

INITIAL CONDITIONS

The solution is started at the beginning of the injection region. Referring to figure 2, this location corresponds to the values X = 18.532 cm, s = 27.292 cm and r_o = 15.951 cm. Initial conditions for the gas (air) and spray are required at this point.

1. Gas

The injection location given above is within the supersonic portion of the flow field. The flow parameters along this initial line (normal to the body) are assumed to have the same values as those calculated at this location without injection. The initial values were obtained from the results of inviscid, streamtube method calculations performed at the NASA Langley

Research Center for the RAM C vehicle (ref. 14). These calculations included non-equilibrium chemistry along the streamlines. For the RAM C vehicle flying at zero angle of attack at 233,000 ft and with free stream conditions of $T_\infty = 205^\circ K$, $p_\infty = 5.042 \times 10^{-5}$ ATM, $V_\infty = 25{,}920$ ft/sec, the flow field results are tabulated in Table 1. The initial shock wave angle is $\nu = 63.236^\circ$. The normal component u_n of the gas velocity V_g was approximated by $u_n = z^3 u_{n\delta}$, and the values of u_s were calculated from the given values of V_g using the relation $V_g^2 = u_s^2 + u_n^2$.

2. Spray

At the initial line $\epsilon = 0$, and to start the calculation it was assumed that at $s = s_o$, $\frac{d\epsilon}{ds} = \tan \phi$.

RESULTS AND DISCUSSION

A fourth-order Runge-Kutta scheme was used in integrating the governing equations and the computations were carried out on an IBM SYSTEM 360/MOD 75 electronic computer. The integration step-size at any stage of the calculation was automatically selected to satisfy a pre-determined accuracy criterion.

A parametric study was carried out to determine the effects of the injection velocity, mass flow rate and drop size, on the flow field. The independent parameters obtained from the governing equations are the dimensionless constants $\beta_1 - \beta_7$ (see Appendix A). Additional parameters are the injected mass flow rate and the injection angle ϕ.

The mass flow rate over the injection distance $s_2 - s_o$ is given by

$$\dot{\bar{m}}_p = 2\pi \rho_{g\infty} V_{g\infty} D_N^2 \beta_2 \beta_3 \int_{s_o}^{s_2} r_o \rho_{po} v_{no} ds \qquad (75)$$

where the superscript bar denotes a dimensional quantity. The injection length $s_2 - s_o$ includes the uniform injection region $s_o \leq s \leq s_1$ and the transition injection region $s_1 \leq s \leq s_2$. A normalized mass flow rate is defined as $\dot{M} = \dot{\bar{m}}_p / \dot{\bar{m}}_g$. Here, $\dot{\bar{m}}_g = \rho_{g\infty} V_{g\infty} \pi D_N^2/4$ is the free stream gas flow rate through the reference area $\pi D_N^2/4$, where D_N is the body nose diameter. Combining the expressions for $\dot{\bar{m}}_p$ and $\dot{\bar{m}}_g$, one obtains

$$\dot{M} = 8\beta_2\beta_3 \int_{s_o}^{s_2} r_o \rho_{po} v_{no} ds \ . \tag{76}$$

Using equations (49), (59) and (60) for the variation of the injection properties ρ_{po} and v_{no}, the above integral can be evaluated. With good approximation, this result can be expressed as

$$\dot{M} \approx 8\beta_2\beta_3(s_1-s_o)[1 + \frac{(s_2-s_1)}{2(s_1-s_o)}][r_o(s_o) + (\frac{s_1-s_o}{2}) \sin\theta] \ . \tag{77}$$

In the computation, we have used $s_2-s_1 = (s_1-s_o)/2$ so that by defining the injection length $\Delta = s_2-s_o$, one obtains for (77)

$$\dot{M} \simeq \frac{20}{3} \beta_2\beta_3\Delta [r_o(s_o) + \frac{\Delta}{3} \sin\theta] \ . \tag{78}$$

Hence, the injected mass flow rate is characterized by the injection length parameter Δ and the product $\beta_2\beta_3$.

The influence of some of the dimensionless parameters was not investigated in this study; thus, β_1, β_4, β_5 and β_7 were chosen as $\beta_1 = .6723\cdot10^{-4}$, $\beta_4 = .9465\cdot10^{-3}$, $\beta_5 = .2058\cdot10^{-3}$, $\beta_7 = 1.137$. In addition, the results were obtained using the constant injection length $\Delta = .03$. The remaining parameters β_2, β_3, β_6 and ϕ were determined from the values chosen for the injection speed, angle, mass flow rate and drop size. The calculations were carried out for the following parameters: (speed) $\bar{V}_p$ = 350,700 cm/sec; (initial angle) tan ϕ = 1, 3; (mass flow rate) $\beta_2\beta_3$ = 1/2, 1, 3/2; (drop size) $\bar{r}_p$ = 75, 100, 125 μ. The results shown in figures 8-12 are for $\beta_2\beta_3 = 1$, $\bar{V}_p = 350$ cm/sec, $\bar{r}_p = 100\mu$ and tan $\phi = 3$.

Figure 5 shows a plot of the ratio of the shock layer thickness with injection to that without injection. The graph, which is typical of the cases investigated, shows that the influence of injection is small on the shock layer thickness. Thus, figures 6 and 7, which give a plot of ϵ/δ vs. s, summarize the influence of the various injection parameters on penetration. The slight decrease in the shock layer thickness is a result of the lower gas velocity. For a given injection drop size and mass flow rate, figure 6 illustrates the expected result of greater penetration for the higher values of injection speed and angle. However, for this case, the relative effect on the penetration of an increased injection speed is much larger than that of an increased injection angle. In figure 7, at a given injection speed and angle, the penetration is greater for the smaller mass flow rate although the overall difference is very small. Also, this figure shows that greater penetration is obtained with a larger drop size for a given mass flow rate. This is in agreement with Volynsky (ref. 15) who found that the deepest penetration was made

by the largest drops. For the cases investigated, the values of the penetration at a distance .75 ft downstream of the initial injection station varied from a minimum of 8.5 percent to a maximum of 17 percent of the shock layer thickness. These results were obtained for the case where $\beta_2\beta_3 = 1$, $\tan \phi = 1$ and $\bar{r}_p = 75\ \mu$ with the minimum value occurring for $\bar{V}_p = 350$ cm/sec and the maximum for $\bar{V}_p = 700$ cm/sec. Thus, at least for this case, the penetration can be doubled by doubling the injection velocity. In general, the results show that greater penetration can be expected with larger values of injection speed, angle and drop size. However, for the mass flow rates investigated, the penetration was found to be almost independent of the mass flow rate. For a given mass flow rate and injection velocity, a large drop size implies a small number density. However, Evans (ref. 7) indicates that a high number density (large surface area per unit volume) as well as a large penetration may be desirable for alleviation of blackout. In this case, a tradeoff effect must be considered.

Figure 8 compares the inclinations of the gas streamlines for the cases of injection and no injection. It illustrates how the streamlines are deflected as a result of injection; even for the low, spray injection velocity of 350 cm/sec, the flow direction is changed by a factor of more than three. Similarly, Billig (ref. 6) showed the large effect of the normal component of the gas velocity on the calculated penetration of a liquid injected into a $M = 5$ airstream over a flat plate.

Figure 9 is a plot of the tangential gas velocity with and without injection at several locations. Since the normal component of the gas velocity is small compared to the tangential component, this plot is representative of the effect of the spray on the gas velocity. The injection and no injection curves all show that the gas accelerates at the downstream shock locations. For the no injection case, the gas also accelerates at the body and within the shock layer. This is the expected result in an expanding supersonic flow. However, for the injection case, the gas is decelerated at the body and everywhere within the shock layer except near the shock itself. Combining these results with those of figure 8, we see that the spray decelerates the gas as well as deflects it. Further downstream, the effect of the spray diminishes and the gas accelerates throughout the shock layer. Such is the case for the profile shown at the distance 1.2 ft downstream of the initial station. The injection curves also show the discontinuous normal derivatives which were postulated at the interface.

The effect of the spray on the gas temperature is shown in figure 10. Here, the ratio of temperatures with and without injection is plotted vs. distance, and any deviation from the value unity represents the effect of the spray. The initial shock layer temperature profile is given in Table 1. In the presence of injection, the results show a large decrease in the gas temperature along the body. This cooling is very rapid. The temperature decreases from an initial value of approximately 3500°K to a value of about 700°K in about .4 ft distance downstream. It is unlikely that the air is cooled this much by the evaporation. Instead, it is reasoned that the gas

along the body is composed mainly of low temperature water vapor evaporated from the spray.

The exclusion of the correct chemical effects obviously influenced the results obtained for the gas temperature within the shock layer. Here, the increased gas temperature can partly be explained by the deacceleration of the gas, and the assumption of frozen chemistry employed here. The curve at the distance 1.2 ft downstream represents approximately the highest temperatures obtained for the specified injection conditions. Temperatures obtained downstream indicate a gradual cooling of the gas.

Figure 11 shows that the smallest drop sizes are obtained along the interface. Within the interface region, the gas temperature is highest at the interface, and the evaporation rate is fastest there. The drop size at the interface decreases by 60 percent in a distance of one foot beyond the injection region. This decrease occurs in approximately $7 \cdot 10^{-3}$ seconds. The figure also shows that very little evaporation occurs at the body; this is due to the low gas temperatures.

The profiles of the spray density are shown in figure 12. The density is essentially uniform at the end of the injection region (s = .925 ft). Downstream of the injection region the density at the body decreases rapidly. The spray density along the body, is influenced by the value of $\left(\frac{\partial \bar{v}_n}{\partial \bar{n}}\right)_0$ which is assumed equal to $\left(\frac{\partial \bar{u}_n}{\partial \bar{n}}\right)_0$ in the no-injection region. The injection causes the gas to be deflected and this derivative is increased in the vicinity of the injection region. The value decreases downstream as the gas flow becomes more nearly parallel to the body. For this reason, the rate of decrease of the spray density at the body is not as large downstream. At the interface, the smallest spray density is obtained because the drop size is smallest at this location. In general, the spray density decreases throughout the interface region as the drops spread into the gas and are accelerated.

In the absence of detailed measurements in the shock layer, the above theory can be checked in two different ways: The first is to compare the predicted penetration with experiment. The second is to use the results from this calculation in a way similar to that employed by Evans (ref. 7) to study the effects of liquid injection on communications blackout. Water injection experiments for the geometry under consideration were carried out by Weaver (ref. 16) using injection velocities which were at least five times higher than the maximum velocity investigated here. Because of the frozen chemistry assumption, use of higher injection velocities would result in temperatures which would be even higher than those indicated in figure 10. Since such temperatures are not realistic, no attempt was made to carry the calculations for higher injection velocities. Thus, meaningful comparison with Weaver's experiments and with data on communications blackout cannot be made at this stage and should await calculations in which the assumption of frozen chemistry is relaxed.

CONCLUSIONS

An analysis is presented for the injection of a liquid spray into a supersonic air flow. The results show that greater penetration is obtained for the higher values of injection speed, angle and drop size. In general, the spray acts to slow and deflect the air with a subsequent rise in the air temperature. The deflection of the air stream enhances the penetration. On the other hand, the increased air temperature results in more evaporation and this tends to lower the penetration because of the reduced drop size. The results of the calculations indicate that the influence of the gas deflection on penetration is more pronounced.

As a result of the initial slowing of the air stream, the assumption of frozen chemistry is questionable. This explains the high temperatures calculated in the shock layer. However, the velocity field is believed to be more representative of actual conditions because the chemistry does not have as great an influence.

With the exception of the gas temperature, it is believed that the method presented here gives reasonably accurate penetration and flow field results. Use of finite chemical reaction rates will result in more accurate flow fields.

North Carolina State University
Raleigh, N. C., December 30, 1967

APPENDICES

APPENDIX A
DERIVATION OF EQUATIONS

Introduction

The equations derived in this appendix are those governing the interaction of a liquid spray and a gas flow. The gas flow is assumed to be inviscid except for the drag it exerts on the droplets of the spray.

The liquid is injected transverse to the air flow, a process which is assumed to result in the production of a very large number of droplets, or spray. Only a statistical description of the spray is feasible, and the necessary spray statistics have been presented by Williams (ref. 9).

Spray Statistics

Droplet Size and Shape. The liquid drops are assumed to be spherical so that the specification of the drop radius is sufficient to completely determine the size and shape of a drop. However, the liquid drops of a spray moving relative to a gaseous medium will be spherical only if the spray is dilute and if the droplet Weber numbers are sufficiently low. In a dilute spray the collisions between drops are infrequent and the ratio of the volume occupied by the drops to the volume occupied by the gas is small. The Weber number is given by

$$W_e = \frac{2 r_p \rho_g |\vec{V}_g - \vec{V}_p|^2}{\sigma_p} \tag{1A}$$

where the subscript p denotes drops and g denotes gas and r, ρ, V and σ are the radius, density, velocity and surface tension, respectively. The Weber number indicates the degree of deformation and the amplitude of oscillation of a liquid drop. In order to have dynamically stable spherical drops, it is necessary that $W_e < 10$, Lane (ref. 17) and Haas (ref. 18). For the gas conditions employed here, this implies a drop radius less than 125 μ ($1\mu = 10^{-4}$ cm). The relative velocity between drops and gas tends to decrease downstream of the point of injection, and the drop radius decreases as a result of evaporation; therefore, drops initially having Weber numbers satisfying $W_e < 10$ will meet this condition throughout.

Distribution Function. Statistically, the spray is described by a distribution function, $f(r_p, \vec{X}, \vec{V}_p, t)$. The quantity

$$f(r_p, \vec{X}, \vec{V}_p, t)\, dr_p d\vec{X} d\vec{V}_p \tag{2A}$$

is the probable number of drops in the radius range dr_p, about r_p located in the spatial range dX, about X with velocities in the range dV_p, about V_p and at time t. Employing reasoning analogous to the kinetic theory of gases, Williams derived the following equation governing the time rate of change of the distribution function, f:

$$\frac{\partial f}{\partial t} = - \frac{\partial (R'f)}{\partial r_p} - \nabla_x \cdot (\vec{V}_p f) - \nabla_v \cdot (\vec{F} f) + Q + \Gamma \, . \tag{3A}$$

Contributions to the rate of change of f due to the terms Q (nucleation and breakup) and Γ (drop collisions) are assumed negligible in the present analysis. In addition the analysis is restricted to the steady state so that the relevant spray equation becomes

$$\frac{\partial (R'f)}{\partial r_p} + \nabla_x \cdot (\vec{V}_p f) + \nabla_v \cdot (\vec{F} f) = 0 \tag{4A}$$

where the force per unit mass acting on a drop at $(r_p, \vec{X}, \vec{V}_p, t)$ is denoted by $\vec{F} = d\vec{V}_p/dt$, and the rate of change of size of a drop at $(r_p, \vec{X}, \vec{V}_p, t)$ is defined as $R' = dr_p/dt$. Expressions for R' and $\vec{F}$ are developed in Appendices B and C, respectively. The vector operator subscripts x and v denote derivatives with respect to spacial and velocity coordinates, respectively.

Spray Equations

The equations used to describe the spray are the mass and momentum conservation equations, an equation relating the change in drop size due to evaporation and an energy equation which reflects the heat exchange necessary to maintain the evaporation. These equations are derived as follows.

Equation of Change. As a first step in the derivation of the conservation equations, the equation of change will be derived. Thus, multiplying equation (4A) by $\phi = \phi (r_p, \vec{V}_p)$ and integrating, one finds that

$$\int_{\vec{V}_p} \int_{r_p} \phi \frac{\partial (R'f)}{\partial r_p} dr_p \, d\vec{V}_p + \int_{\vec{V}_p} \int_{r_p} \phi \nabla_x \cdot (\vec{V}_p f) dr_p d\vec{V}_p$$

$$+ \int_{\vec{V}_p} \int_{r_p} \phi \nabla_v \cdot (\vec{F} f) dr_p d\vec{V}_p = 0 \tag{5A}$$

where $\int_{\vec{V}_p} \int_{r_p} \equiv \int_{-\infty}^{\infty} \int_{0}^{\infty}$ and ϕ can be either a scalar or vector function.

The first integral can be integrated by parts with respect to r_p to give

$$\int_{\bar{V}_p}\int_{r_p} \phi \frac{\partial(R'f)}{\partial r_p} dr_p d\vec{V}_p = \int_{-\infty}^{\infty} [(\phi R'f)\Big|_0^{\infty} - \int_0^{\infty} R'f \frac{\partial \phi}{\partial r_p}] d\vec{V}_p \ . \tag{6A}$$

However, $f \longrightarrow 0$ when $r_p \longrightarrow 0, \infty$ and as a result $(\phi R'f)\Big|_0^{\infty} = 0$ so that

$$\int_{\vec{V}_p}\int_{r_p} \phi \frac{\partial(R'f)}{\partial r_p} dr_p d\vec{V}_p = -\int_{-\infty}^{\infty}\int_0^{\infty} R'f \frac{\partial \phi}{\partial r_p} dr_p d\vec{V}_p \ . \tag{7A}$$

Since r_p, $\vec{X}$ and $\vec{V}_p$ are all independent variables, the second integral of (5A) can be written as

$$\int_{\vec{V}_p}\int_{r_p} \phi \nabla_x \cdot (\vec{V}_p f) dr_p d\vec{V}_p = \nabla_x \cdot \int_{-\infty}^{\infty}\int_0^{\infty} \phi \vec{V}_p f dr_p d\vec{V}_p \tag{8A}$$

if ϕ is a scalar function, and if $\phi = \vec{\phi}$ is a vector function as

$$\int_{\vec{V}_p}\int_{r_p} \vec{\phi} \nabla_x \cdot (\vec{V}_p f) dr_p d\vec{V}_p = \nabla_x \cdot \int_{-\infty}^{\infty}\int_0^{\infty} (\vec{\phi};\vec{V}_p) f dr_p d\vec{V}_p \tag{9A}$$

where $\vec{\phi};\vec{V}_p$ is a dyadic product.

When ϕ is a scalar, the third integral of (5A) reduces to

$$\int_{\vec{V}_p}\int_{r_p} \phi \nabla_v \cdot (\vec{F} f) dr_p d\vec{V}_p = \int_{-\infty}^{\infty}\int_0^{\infty} \nabla_v \cdot (\phi \vec{F} f) dr_p d\vec{V}_p$$

$$- \int_{-\infty}^{\infty}\int_0^{\infty} [\vec{F} \cdot (\nabla_v \phi)] f dr_p d\vec{V}_p \tag{10A}$$

and when $\phi = \vec{\phi}$, it becomes

$$\int_{\vec{V}_p}\int_{r_p} \vec{\phi} \nabla_v \cdot (\vec{F} f) dr_p d\vec{V}_p = \int_{-\infty}^{\infty}\int_0^{\infty} \nabla_v \cdot [(\vec{\phi};\vec{F}) f] dr_p d\vec{V}_p$$

$$- \int_{-\infty}^{\infty}\int_0^{\infty} [(\vec{F} \cdot \nabla_v)\vec{\phi}] f dr_p d\vec{V}_p \ . \tag{11A}$$

The first integral on the right in (10A) and (11A) can be shown to vanish when integrated over $\bar{V}_p$ by using the divergence theorem and the fact that $f \longrightarrow 0$ when $V_p \longrightarrow \pm \infty$. Equations (10A) and (11A) then become

$$\int_{\vec{V}_p}\int_{r_p} \phi\,\nabla_v\cdot(\vec{F}f)\,dr_p d\vec{V}_p = -\int_{-\infty}^{\infty}\int_{0}^{\infty} [\vec{F}\cdot(\nabla_v\phi)]f\,dr_p d\vec{V}_p \qquad (12A)$$

and

$$\int_{\vec{V}_p}\int_{r_p} \vec{\phi}\nabla_v\cdot(\vec{F}f)\,dr_p d\vec{V}_p = -\int_{-\infty}^{\infty}\int_{0}^{\infty} [(\vec{F}\cdot\nabla_v)\vec{\phi}]f\,dr_p d\vec{V}_p \,. \qquad (13A)$$

Combining the results (7A), (8A), (9A), (12A) and (13A), the equation of change for the general spray property ϕ, is given by

$$-\int_{-\infty}^{\infty}\int_{0}^{\infty} R'f\frac{\partial\phi}{\partial r_p}\,dr_p d\vec{V}_p + \nabla_x\cdot\int_{-\infty}^{\infty}\int_{0}^{\infty}\phi\vec{V}_p f\,dr_p d\bar{V}_p$$

$$-\int_{-\infty}^{\infty}\int_{0}^{\infty}[\vec{F}\cdot(\nabla_v\phi)]f\,dr_p d\vec{V}_p = 0 \qquad (14A)$$

when ϕ is a scalar, and by

$$-\int_{-\infty}^{\infty}\int_{0}^{\infty} R'f\frac{\partial\vec{\phi}}{\partial r_p}\,dr_p d\vec{V}_p + \nabla_x\cdot\int_{-\infty}^{\infty}\int_{0}^{\infty}(\vec{\phi};\vec{V}_p)f\,dr_p d\vec{V}_p$$

$$-\int_{-\infty}^{\infty}\int_{0}^{\infty}[(\vec{F}\cdot\nabla_v)\vec{\phi}]f\,dr_p d\vec{V}_p = 0 \qquad (15A)$$

when $\phi = \vec{\phi}$.

In order to simplify the evaluation of the integrals appearing in (14A) and (15A), it is assumed that

$$f(r_p,\vec{X},\vec{V}_p) = g(r_p,\vec{X})\,\delta_D(\vec{V}_p-\bar{\vec{V}}_p) \qquad (16A)$$

which serves to define the size distribution function g and where δ_D is the three-dimensional Dirac-delta function with the property that $\int_{\bar{V}_p}\delta_D(\vec{V}_p-\bar{\vec{V}}_p)d\vec{V}_p$ = 1, provided that $\vec{V}_p = \bar{\vec{V}}_p$ is in the range of integration and zero otherwise. Here, $\bar{\vec{V}}_p$ is meant to represent the locally average value of the drop velocities.

Continuity. Here, $\phi = 4\pi r_p^3 m_p/3$ is the mass of a drop, where m_p is the material density of the drop. Thus, $\partial\phi/\partial r_p = 4\pi r_p^2 m_p$ and $\nabla_v \phi = 0$. Using (16A) in (14A) it can be shown that

$$\nabla_x \cdot \bar{\vec{V}}_p \int_0^\infty \frac{4}{3} \pi r_p^3 m_p \, g \, dr_p = \int_0^\infty 4\pi r_p^2 m_p \, \bar{R}' g \, dr_p \tag{17A}$$

where $\bar{R}'$ denotes R' evaluated at $\vec{V}_p = \bar{\vec{V}}_p$. However, the mass of condensed phase per unit spatial volume is given by

$$\rho_p \equiv \int_0^\infty \frac{4}{3} \pi r_p^3 m_p \, g \, dr_p \tag{18A}$$

and ρ_p will be called the spray density. It follows from equations (17A) and (18A) that the continuity equation for the spray can be written as

$$\nabla_x \cdot (\rho_p \bar{\vec{V}}_p) = \int_0^\infty 4\pi r_p^2 m_p \, \bar{R}' \, g \, dr_p \, . \tag{19A}$$

Momentum. Here, $\vec{\phi} = \frac{4}{3} \pi r_p^3 m_p \vec{V}_p$ is the momentum of a drop. Thus, $\partial\vec{\phi}/\partial r_p = 4\pi r_p^2 m_p \vec{V}_p$ and $(\vec{F} \cdot \nabla_v)\vec{\phi} = \frac{4}{3} \pi r_p^3 m_p \vec{F}$. Using (16A) the integrations over $\bar{V}_p$ in (15A) can be carried out, giving

$$-\bar{\vec{V}}_p \int_0^\infty 4\pi r_p^2 m_p \, \bar{R}' \, g \, dr_p + \nabla_x \cdot (\bar{\vec{V}}_p ; \bar{\vec{V}}_p) \int_0^\infty \frac{4}{3} \pi r_p^3 m_p \, g \, dr_p$$

$$- \int_0^\infty \frac{4}{3} \pi r_p^3 m_p \bar{\vec{F}} \, g \, dr_p = 0 \tag{20A}$$

where $\bar{\vec{F}}$ represents $\vec{F}$ evaluated at $\vec{V}_p = \bar{\vec{V}}_p$. Using equations (17A) and (18A), equation (20A) reduces to

$$-\bar{\vec{V}}_p \nabla_x \cdot (\rho_p \bar{\vec{V}}_p) + \nabla_x \cdot [(\bar{\vec{V}}_p ; \bar{\vec{V}}_p)\rho_p] - \int_0^\infty \frac{4}{3} \pi r_p^3 m_p \bar{\vec{F}} \, g \, dr_p = 0 \, . \tag{21A}$$

The second term above can be expanded to give

$$\nabla_x \cdot [\rho_p (\bar{\vec{V}}_p ; \bar{\vec{V}}_p)] = \rho_p [(\nabla_x \times \bar{\vec{V}}_p) \times \bar{\vec{V}}_p + \frac{1}{2} \nabla \bar{V}_p^2] + \bar{\vec{V}}_p [\nabla_x \cdot (\rho_p \bar{\vec{V}}_p)] \, . \tag{22A}$$

Substituting (22A) into (21A) and canceling, the following conservation of momentum equation for the spray is obtained:

$$\rho_p[(\nabla_x \times \vec{\bar{V}}_p) \times \vec{\bar{V}}_p + \frac{1}{2}\nabla \vec{V}_p^{\,2}] = \int_0^\infty \frac{4}{3}\pi r_p^{\,3} m_p \vec{\bar{F}}\, g\, dr_p \quad . \tag{23A}$$

Due to the assumed f dependence on $\vec{V}_p$, the pressure contributed by the thermal motion of the drops is necessarily zero; hence, it does not appear in (23A).

Energy. The energy equation for the spray is taken as the statement expressing equilibrium between the heat transferred to the drop from the air and the heat consumed by the drop while evaporating. The drop temperature is assumed uniform. Thus, if $\dot{Q}$ represents the rate of heat transfer to the drop from the surroundings, $\dot{m}$ the steady evaporation rate and L the droplet latent heat of vaporization, the droplet or spray energy equation can be expressed as

$$\dot{Q} = \dot{m}L \quad . \tag{24A}$$

This equation allows the determination of the droplet saturation vapor pressure (or temperature) from the properties of the surrounding gas and the drop size. Expressions for $\dot{m}$ and $\dot{Q}$ are given in Appendix B.

Drop Radius. In addition to the usual conservation equations, it is necessary to describe the rate of change of the drop radius. Introducing the quasi-steady state assumption for the evaporation process (see Appendix B), one can write

$$\dot{m} = -\frac{D}{Dt}\left(\frac{4}{3}\pi r_p^{\,3} m_p\right) = -4\pi r_p^{\,2} m_p) = -4\pi r_p^{\,2} m_p\, (\bar{V}_p \cdot \nabla r_p) \tag{25A}$$

where $D/Dt = \partial/\partial t + \bar{V}_p \cdot \nabla$ is the total derivative. Hence

$$\bar{V}_p \cdot (\nabla r_p) = -\dot{m}/4\pi r_p^{\,2} m_p \quad . \tag{26A}$$

Gas Equations

The conservation equations used for the gas are the ordinary equations of fluid dynamics, with suitably added source terms accounting for the average effect of the spray (ref. 9).

Continuity. The mass per unit volume per second added to the gas from the evaporating spray is

$$\int_{-\infty}^{\infty}\int_0^\infty 4\pi m_p r_p^{\,2} R' f\, dr_p\, d\vec{V}_p \tag{27A}$$

or, integrating with respect to $\vec{V}_p$ and using (16A), the above expression reduces to

$$\int_0^\infty 4\pi m_p r_p^2 \bar{R}' g \, dr_p \, . \tag{28A}$$

The gas continuity equation is then given by

$$\nabla \cdot (\rho_f \vec{V}_g) = -\int_0^\infty 4\pi m_p r_p^2 \bar{R}' g \, dr_p \tag{29A}$$

where ρ_f, called the fluid density, is the mass of gas (air plus liquid vapor) per unit volume of physical space. The amount of liquid vapor relative to the amount of air in a given volume is assumed to be small enough so that the properties for the gas are essentially those of air (Appendix D). Also, the usual density of the gas ρ_g (i.e., the mass of gas per unit volume of space available to the gas) differs from ρ_f because of the volume occupied by the spray. The previous assumption of a dilute spray will be violated whenever ρ_f differs greatly from ρ_g; therefore, the ratio ρ_f/ρ_g, given by

$$\frac{\rho_f}{\rho_g} = 1 - \int_{-\infty}^{\infty} \int_0^\infty \frac{4}{3} \pi r_p^3 f dr_p^3 d\vec{V}_p = 1 - \frac{\rho_p}{m_p} \tag{30A}$$

should be kept small. Henceforth, we will take $\rho_f = \rho_g$. Consequently, the gas continuity equation becomes

$$\nabla \cdot (\rho_g \vec{V}_g) = -\int_0^\infty 4\pi m_p r_p^2 \bar{R}' g \, dr_p \, . \tag{31A}$$

Momentum. Accounting for the drag exerted on the gas by the spray, the time rate of momentum addition to the gas by the spray, and neglecting the viscous terms in the pressure tensor, the equation of conservation of momentum for the gas can be written as

$$\rho_g [(\nabla \times \vec{V}_g) \times \vec{V}_g + \frac{1}{2} \nabla V_g^2] + \nabla p_g = -\int_0^\infty \frac{4}{3} \pi m_p r_p^3 \vec{\bar{F}} g \, dr_p$$

$$+ (\vec{V}_g - \vec{\bar{V}}_p) \int_0^\infty 4\pi m_p r_p^2 \bar{R}' g \, dr_p \, . \tag{32A}$$

The first integral represents the force per unit volume exerted on the gas by the spray while the second integral accounts for the momentum carried to the gas by the vapor evaporating from the spray. The hydrostatic pressure of the gas is given by p_g.

Energy. Following Williams (ref. 9), the gas energy equation may be taken as

$$\nabla\cdot[\rho_g \vec{V}_g (h_g + \frac{V_g^2}{2})] = -\int_0^\infty \frac{4}{3}\pi r_p^3 m_p (\vec{\bar{F}}\cdot\vec{\bar{V}}_p)\, g\, dr_p$$

$$- \int_0^\infty 4\pi r_p^2 m_p \bar{R}' (h_p + \frac{\bar{V}_p^2}{2})\, g\, dr_p \,. \qquad (33A)$$

In deriving this equation the heat flux vector in the gas has been taken as zero and all viscous terms have been excluded. Here, h_g is the specific enthalpy of the gas and h_p is the enthalpy flowing to the gas per unit mass of vapor. The first integral gives the work done on the gas by the spray while the second integral denotes the energy added to the gas by the evaporating spray.

State. Neglecting the partial pressure of the vapor and assuming the air to be a mixture of ideal gases, the equation of state for the gas is given by

$$p_g = \rho_g \frac{R_o}{M_g} T_g \qquad (34A)$$

where R_o is the universal gas constant, T_g the gas temperature and M_g is the mixture molecular weight, defined for an N component mixture by

$$M_g = \sum_{i=1}^{N} X_i M_i, \quad X_i = \text{mole fraction} \,. \qquad (35A)$$

The equations given by (19A), (23A), (26A), (31A), (32A) and (33A) constitute a set of coupled integrodifferential equations. Solution of this set along with the supplemental equations (24A) and (34A) is very complicated and very laborious. To alleviate this untenuable position, certain simplifying assumptions must be made in the equations. As a first step in this direction, the following section will introduce assumptions allowing one to evaluate the integrals appearing in these equations; thus, the set of integrodifferential equations are replaced by a corresponding set of approximating differential equations.

Explicit Expressions for the Source Term Integrals

The distribution function has already been assumed to have the form

$$f = g(r_p, \vec{X})\, \delta_D (\vec{V}_p - \vec{\bar{V}}_p) \qquad (16A)$$

with $\vec{\bar{V}}_p$ representing the average (local) velocity of the spray droplets and

where $g(r_p,\vec{X})$ is the size distribution function. It is now assumed that the spray also may be represented by an average drop size, $r_p = \bar{r}_p$; therefore, we take

$$g(r_p,\vec{X}) = n(\vec{X})\ \delta_D\ (r_p-\bar{r}_p) \tag{36A}$$

where $n(\vec{X})$ is the number density of drops in the spray and δ_D again represents the Dirac-delta function. The integrals over r_p appearing in the spray and gas equations can now be evaluated giving the following results:

$$\int_0^\infty 4\delta m_p r_p^2\ \bar{R}'\ g\ dr_p = \frac{3\bar{R}'\rho_p}{\bar{r}_p}$$

$$\int_0^\infty \frac{4}{3}\ \delta m_p r_p^3\ \bar{\vec{F}}\ g\ dr_p = \rho_p \bar{\vec{F}}$$

$$\int_0^\infty \frac{4}{3}\ \delta m_p r_p^3 (\bar{\vec{F}}\cdot\bar{\vec{V}}_p)\ g\ dr_p = \rho_p (\bar{\vec{F}}\cdot\bar{\vec{V}}_p) \tag{37A}$$

$$(h_p + \frac{\bar{V}_p^2}{2}) \int_0^\infty 4\delta m_p r_p^2\ \bar{R}'\ g\ dr_p = \frac{3\bar{R}'\rho_p}{\bar{r}_p}\ (h_p + \frac{\bar{V}_p^2}{2})$$

Here, $\bar{R}'$ and $\bar{\vec{F}}$ now represent values evaluated at the average value $\bar{r}_p$ as well as at $\bar{\vec{V}}_p$.

Dimensionless Governing Equations

The spray and gas equations are normalized using the definitions given in Appendix E. Use is made of the expressions for $\dot{Q}$ and $\dot{m}$ and R' from Appendix B and for $\bar{F}$ from Appendix C. In addition, the superscript bars denoting average values are dropped and the dimensionless variables are expressed in the heretofore dimensional notation. The following dimensionless governing equations for the spray and the gas result:

Spray Continuity.

$$\nabla\cdot(\rho_p\vec{V}_p) = -3\ \frac{\beta_1\beta_5\beta_6^2}{\beta_2}\ \frac{\rho_p\chi}{r_p^2} \tag{38A}$$

where $\chi = \frac{p_0 D}{T_p}\left[\frac{2\Delta}{\alpha r_p} + \frac{r_p}{r_p+\Delta}\right]^{-1}$.

Spray Momentum.

$$\left(\nabla X \vec{V}_p\right) X \vec{V}_p + \frac{1}{2}\nabla V_p^2 = \frac{3}{8}\frac{\beta_5\beta_6}{\beta_2^2}\frac{\rho_g C_D}{r_p}\left(\vec{V}_g - \beta_2\vec{V}_p\right)\left|\vec{V}_g - \beta_2\vec{V}_p\right| . \tag{39A}$$

Spray Energy.

$$p_0 = \frac{\lambda_g T_p}{L D}\left(T_g - \beta_7 T_p\right)\frac{\left[\frac{2\Delta}{\alpha r_p} + \frac{r_p}{r_p+\Delta}\right]}{\left[\frac{2\Delta_T}{\alpha_T r_p} + \frac{r_p}{r_p+\Delta_T}\right]} . \tag{40A}$$

Drop Radius.

$$\vec{V}_p \cdot \left(\nabla r_p\right) = -\frac{\beta_1\beta_5\beta_6^2}{\beta_2}\frac{\chi}{r_p} . \tag{41A}$$

Gas Continuity.

$$\nabla \cdot \left(\rho_g \vec{V}_g\right) = 3\beta_1\beta_3\beta_5\beta_6^2\frac{\rho_p}{r_p^2}\chi . \tag{42A}$$

Gas Momentum.

$$\left(\nabla X \vec{V}_g\right) X \vec{V}_g + \frac{1}{2}\nabla V_g^2 + \frac{\beta_4}{\rho_g}\nabla p_g = -3\beta_3\beta_5\beta_6\frac{\rho_p}{\rho_g r_p}\left(\vec{V}_g - \beta_2\vec{V}_p\right)$$

$$\cdot\left[\frac{\rho_g C_D}{8}\left|\vec{V}_g - \beta_2\vec{V}_p\right| + \beta_1\beta_6\frac{\chi}{r_p}\right] . \tag{43A}$$

Gas Energy.

$$\nabla\cdot[\rho_g\vec{V}_g(h_g+\frac{V_g^2}{2})] = -3\beta_2\beta_3\beta_5\beta_6\frac{\rho_p}{r_p}[\frac{\rho_g C_D}{8}|\vec{V}_g-\beta_2\vec{V}_p|(\vec{V}_g-\beta_2\vec{V}_p)\cdot\vec{V}_p$$

$$-\beta_1\beta_2\beta_6\frac{\chi}{r_p}(h_p+\frac{V_p^2}{2})] \quad . \tag{44A}$$

State.

$$p_g = Z_c\rho_g T_g \quad . \tag{45A}$$

The dimensionless parameters (denoted by the β's) appearing in the above equations are defined as

$$\beta_1 = \frac{\mu_{g_\infty}}{\rho_{g_\infty} V_{g_\infty} D_N} = \frac{1}{Re_\infty} \quad , \quad \beta_2 = \frac{v_{n\text{-}inj}}{V_{g_\infty}} \quad , \quad \beta_3 = \frac{\rho_{p\text{-}inj}}{\rho_{g_\infty}} \quad ,$$

$$\beta_4 = \frac{1}{\gamma_\infty M_\infty^2} \quad , \quad \beta_5 = \frac{\rho_{g_\infty}}{m_p} \quad , \quad \beta_6 = \frac{D_N}{r_{p\text{-}inj}} \quad , \quad \beta_7 = \frac{T_{p\text{-}ref}}{T_{g_\infty}} \quad . \tag{46A}$$

APPENDIX B
EVAPORATION

Introduction

The evaporation of a spray injected into the high-speed, high-temperature environment of a reentry vehicle is a very complicated process. Calculations for the size and temperature histories of the spray droplets cannot be performed unless many assumptions are introduced in the actual physical model. The following sections will present the assumptions employed and the resulting expressions used for calculating the evaporation rate of the spray.

Theory

Physical Environment. As a starting point in the spray evaporation analysis, we use the previously given assumption (Appendix A) that the injection process results in a large number of dynamically stable, spherical droplets. From Williams (ref. 9), the time rate of change of diameter of a drop depends on the physicochemical evaporation process and on the nature of the surrounding environment. For sufficiently slow changes in the drop size and in the environment, the time dependent terms in the governing equations may be dropped and the quasi-steady-state evaporation rates may be employed. Thus, the time dependence of the evaporation only enters through changes in the ambient conditions and drop diameter; that is, the steady-state solution obtained for a fixed drop size applies to the evaporating drop when it reaches the diameter used in the steady-state solution. This assumption greatly simplifies the mathematical treatment.

Consistent with the statistical assumptions introduced in Appendix A, it is assumed that the spray evaporation can be determined from the known evaporative properties of representative droplets. Hence, we seek to describe the evaporation of a single drop in the shock layer. The Re number for the largest drops considered in this work is small so that the appropriate rarefaction parameter for the droplets is the Mach number to Reynolds number ratio, $M/Re = \mu_\infty / a_\infty \rho_\infty d$, where d, μ_∞, a_∞ and ρ_∞ are the droplet diameter, viscosity, speed of sound and density of the gas at large distances from the drop, respectively. The injection considered in this work is into the expanding, supersonic portion of the shock layer, and the evaporating drops should experience a minimum value of the ratio M/Re when at their maximum diameter corresponding to the injection values. The maximum diameter at which drops can be injected into the given environment has already been shown (Appendix A) to be approximately 250 μ. Consequently, an approximate lower limit for the ratio M/Re occurs for the drops when they are first injected and is of the order $M/Re \approx 1$. Since the range, $.01 < M/Re < \infty$, includes both the transition and free-molecule regimes, Schaaf and Chambre (ref. 19), allowances for rarefaction effects must be made in the droplet evaporation analysis. Deviations from continuum evaporation theory in the absence of convection effects will occur whenever the drop radius is comparable with the mean free path of a

vapor molecule; thus, continuum results are not applicable to either small droplets at moderate pressures or to larger droplets at lower pressures, (ref. 20).

If no convection currents are present, continuum droplet evaporation theory hinges on the diffusion of vapor molecules away from the drop and the influx of heat into the drop, (ref. 20). Most theoretical treatments consider evaporation as a problem with quasi-steady gradients of composition and temperature, and then make assumptions regarding the variation of the relevant properties (e.g., diffusion coefficient, thermal conductivity) over the gradients (ref. 21). In the presence of large temperature and concentration gradients, the mass diffusion and heat transfers have an appreciable effect on each other and cannot be decoupled as is done in many treatments. Indeed, this case, as pointed out by Fuchs (ref. 22), requires a special detailed analysis which so far has not been carried out.

Diffusional control of evaporation will diminish as the drop decreases in size; in the limit of very small drops, the evaporation is kinetically controlled and proceeds as if in a vacuum. Following Kennard (ref. 23), a drop surrounded by its saturated vapor will undergo equal rates of evaporation and condensation. The evaporation rate for this case can easily be calculated since it is exactly equal to the condensation rate which can be determined from the known number of molecules per unit area per unit time striking the droplet surface. To explain the net or observed evaporation (or condensation) which occurs when there is an imbalance in these rates, an unknown factor α is introduced which represents the fraction of impinging vapor molecules that do condense.

For evaporating drops moving relative to the surrounding medium, consideration must be given to the forced convective effects which are present. Mathematical difficulties have not as yet allowed the complete solution for all Reynolds numbers for the rates of evaporation or heat transfer from a spherical body ventilated by a gas stream. The approximations which have appeared are limited to particular Reynolds number ranges, (ref. 22). However, as pointed out by Fuchs, for drops moving relative to a high-speed, rarefied gaseous medium, the width of the diffusion boundary layer is less than the mean free path of the vapor molecules and practically all the evaporating molecules will be carried away by the gas; i.e., evaporation will proceed as if in a vacuum. In this work, as a first approximation, the effects of convection will be ignored, an approximation which should be of increasing validity because the evaporation rate so derived tends toward the correct vacuum rate. If, as expected, the rates of mass and heat transfer are increased by the effects of convection currents, (ref. 24), neglecting convective effects should yield results representing a lower limit for the actual process.

Evaporation with $\ell/r_p \ll 1$. Consider the steady evaporation of a motionless, spherical drop into a gaseous medium with uniform temperature and pressure but with nonuniform vapor concentration. If the drop radius, r_p, is considerably larger than the mean free path, ℓ, of a vapor molecule and the equilibrium vapor pressure of the material is considerably less than the total

pressure of the medium, the evaporation rate (mass/time) is given by Maxwell's formula, (ref. 22)

$$\dot{m}_o = 4\pi r_p D(c_o - c_\infty) \tag{1B}$$

where D, c_o and c_∞ are the diffusion coefficient of the vapor, vapor concentration (mass/volume) in equilibrium with the droplet and vapor concentration at large distance from the drop, respectively. When $c_o < c_\infty$, we have condensation and when $c_o > c_\infty$ we have evaporation. When $c_o = c_\infty$, equilibrium exists with no net evaporation or condensation occurring. One exception to this condition occurs for small drops in a medium saturated with vapor. In this case evaporation does take place due to the increased vapor pressure of the drops owing to their curved surfaces. For a drop of radius r_p and temperature T, the vapor pressure will be increased over the ordinary value for a flat liquid surface at the same temperature in accordance with the Kelvin equation, ref. (22) and (25)

$$\ln \frac{p_o}{p_\infty} = \frac{2\sigma}{r_p R T m_p} \quad \text{or} \quad \frac{p_o - p_\infty}{p_\infty} = \frac{2\sigma}{r_p R T m_p} \tag{2B}$$

where p_o is the vapor pressure of the drop at temperature T, p_∞ the vapor pressure over a flat liquid surface at the same temperature, σ the surface tension, m_p the liquid density and R the gas constant of the vapor. Because of this elevation in vapor pressure, any water droplet, unless extremely large, will evaporate in air of 100 percent humidity, (ref. 20). However, except for extremely small droplets, the effect is small.

Corrections to Maxwell's formula must be made if the concentration of the evaporating vapor is not small compared to the concentration of the surrounding medium, (ref. 21). Fuchs (ref. 22) has shown that the evaporation rate when allowing for this so-called "Stefan flow" should be expressed as

$$\dot{m} = \dot{m}_o \left(1 + \frac{p_o + p_\infty}{2P}\right) \tag{3B}$$

where $\dot{m}_o$ is the evaporation rate according to Maxwell, P the total pressure of the medium, p_o and p_∞ are the partial vapor pressures in equilibrium with the droplet surface and at large distance from the drop, respectively. Generally, this correction is small within the range of conditions for which Maxwell's equation holds.

Evaporation with Arbitrary ℓ/r_p. When the drop radius is of the same order as the mean free path of the vapor, the simple diffusion theory given in the preceding section breaks down. Analogous to the familiar viscous slip and

temperature jump arising at the interface between two phases, Langmuir (ref. 26) pointed out the existence of a rapid change in vapor concentration at the surface of an evaporating drop. Maxwell's equation assumes that the macroscopic diffusion equation may be applied right up to the surface of the drop which is surrounded by saturated vapor, an assumption which does not hold if $\ell \approx r_p$. Fuchs (ref. 27) derived an equation correcting Maxwell's formula for the abrupt change of concentration of a drop of any radius. The corrections were obtained by assuming that the rate of removal of vapor by diffusion as given by Maxwell's formula can be applied only at distances Δ, of the order of ℓ, from the surface of the drop, while in the region between the drop surface and Δ, the transfer of vapor molecules occurs as in a vacuum. In this latter region, the net rate of evaporation is given by

$$\dot{m} = 4\pi r_p^2 \nu\alpha(c_0 - c_1) \tag{4B}$$

where c_1 is the vapor concentration at a distance Δ from the drop, ν is one-fourth of the mean speed of a vapor molecule and α is the evaporation coefficient, assumed equal to the previously defined condensation coefficient. Equating this rate to Maxwell's rate at a distance Δ from the drop

$$\dot{m} = 4\,(r_p + \Delta)(c_1 - c_\infty) \tag{5B}$$

and eliminating the concentration c_1, there results

$$\dot{m} = \frac{\dot{m}_o}{\left[\left(\frac{D}{r_p \nu\alpha}\right) + \left(\frac{r_p}{r_p + \Delta}\right)\right]} \tag{6B}$$

which tends to Maxwell's formula (1B) if r_p is large and to the vacuum rate, $4\pi r_p^2 \nu\alpha c_o$, if r is small. Explicit expressions for Δ are discussed by Wright, (ref. 28).

Evaporation with Heat Transfer. Under conditions of steady evaporation, the quantity of heat transferred to the drop must equal the amount needed to supply the latent heat of vaporization consumed in the evaporation, i.e.

$$\dot{Q} = L\dot{m} \tag{7B}$$

where $\dot{Q}$ is the heat rate to the drop and L the latent heat of vaporization of the liquid. As a consequence of this heat transfer, the temperature of the drop must be less than the gas surrounding it; this process is usually referred to as the self-cooling of the evaporating drop. Neglecting heat transfer by radiation and convection and assuming the thermal conductivity of the medium to be constant, the heat transferred to the drop is given by

$$\dot{Q} = 4\pi r_p \lambda(T_\infty - T_0) \tag{8B}$$

where λ is the thermal conductivity, T_∞ the temperature of the gaseous medium at large distance from the drop and T_0 the droplet temperature. Using equations (1B), (7B) and (8B), Fuchs (ref. 22) obtained the expression

$$T_\infty - T_0 = \frac{LD}{R\lambda}\left(\frac{p_o}{T_0} - \frac{p_\infty}{T_\infty}\right) \tag{9B}$$

where $p_o = f(T_0)$ is a function of the drop temperature alone, which enables one to calculate T_0 (or p_o) for given conditions p_∞, T_∞. Mason (ref. 29) applied the approximate form of the Clapeyron-Clausius equation (valid provided $T_\infty - T_0$ is small) to account for the effect on the vapor pressure of the self-cooling of the drop, and obtained an expression giving the evaporation rate in terms of the radius of the drop and the liquid vapor pressure evaluated at the temperature of the surrounding medium. Equation (8B) is not applicable whenever $\ell \approx r_p$ and must be corrected for the temperature change at the droplet surface, analogous to the concentration change. Wright (ref. 21), in a paper intended to account for the effect of heat transfer on the evaporation rate of arbitrarily small droplets, followed the evaporation model of Fuchs (ref. 27) and introduced a thermal analogue, Δ_T, to the Δ of Fuchs. He considered evaporation into a large excess of gas; thus, practically all of the transport of heat to the drop was due to the molecules of the surrounding gas. An explicit expression for Δ_T was given. Considering the condensation of a supersaturated vapor on a drop in both rarefied and continuum environments, Kang (ref. 30) employed a somewhat similar energy balance model as Wright, but allowed for the transport of heat to the drop by the impinging vapor molecules.

Spray Evaporation Expressions

Expressions for the spray evaporation into the environment presented by the shock layer will be developed in this section. The basic plan of attack will be to follow as closely as possible the previously mentioned derivations for the mass and heat transfer for drops of arbitrary radius while relaxing the assumption of uniform temperatures or small gradients whenever possible.

Following the reasoning of Fuchs (ref. 27) for droplets of arbitrary radius, the net evaporation rate in the region $r_p \leq r \leq r_p + \Delta$ can be expressed as

$$\dot{m} = 4\pi r_p^2 \alpha \left[c_o \sqrt{\frac{RT_0}{2\pi}} - c_\Delta \sqrt{\frac{RT_\Delta}{2\pi}}\right] \tag{10B}$$

where c is the concentration and T is the temperature of the vapor, with the subscripts 0 and Δ referring to the drop surface and distance Δ (the Δ of

of Fuchs) from the drop, respectively. Here, R is the gas constant of the vapor and the other symbols have their usual meanings. We wish to equate the above rate to the rate of removal of vapor by diffusion at the distance Δ. According to Wright (ref. 21), the concentration gradient must be expressed in terms of the mole fraction if the temperature is not uniform; therefore, from Penner (ref. 31), we have for a spherically symmetric system

$$\dot{m} = -4\pi r^2 c D \frac{d \ln}{dr} \left(\frac{M}{\bar{M}} X\right) \tag{11B}$$

where M, $\bar{M}$ and X are the vapor molecular weight, mixture molecular weight and vapor mole fraction, respectively. The radial coordinate is denoted by r. Since $c/\bar{c} = MX/\bar{M}$, where $\bar{c}$ is the mixture concentration, we have

$$\dot{m} = -4\pi r^2 \bar{c} D \frac{d}{dr} (MX/\bar{M}) . \tag{12B}$$

Assuming $\bar{c}D$ constant and integrating gives

$$X(r) - X(\infty) = \left(\frac{\bar{M}}{M}\right) \frac{\dot{m}}{4\pi r \bar{c} D} . \tag{13B}$$

Applying the above expression at $r_p + \Delta$ gives

$$\dot{m} = 4\pi (r_p + \Delta) D \left[c_\Delta - \left(\frac{\bar{M}_\infty \bar{c}_\Delta}{\bar{M}_\Delta \bar{c}_\infty}\right) c_\infty\right] \tag{14B}$$

where the subscript Δ denotes values evaluated at $r_p + \Delta$. Equating equations (10B), (14B) and eliminating c_Δ gives

$$\dot{m} = \frac{4\pi r_p D\left[c_o - \left(\sqrt{\frac{T_\Delta}{T_o}} \frac{\bar{M}_\infty \bar{c}_\Delta}{\bar{M}_\Delta \bar{c}_\infty}\right) c_\infty\right]}{\left[\frac{D_\Delta}{r_p \nu_o \alpha} + \left(\frac{r_p}{r_p + \Delta}\right)\sqrt{\frac{T_\Delta}{T_o}}\right]} \tag{15B}$$

where ν_o is one-fourth the mean speed of a vapor molecule at the drop temperature. Using the explicit expression for Δ suggested by Wright (ref. 28), we have

$$\Delta = \frac{D_\Delta}{2\nu_o} \tag{16B}$$

so that

$$\dot{m} = \frac{4\pi r_p D \left[c_o - \left(\sqrt{\frac{T_\Delta}{T_0}}\ \frac{\bar{M}_\infty \bar{c}_\Delta}{\bar{M}_\Delta \bar{c}_\infty}\right) c_\infty\right]}{\left[\frac{2}{\alpha}\frac{\Delta}{r_p} + \sqrt{\frac{T_\Delta}{T_0}}\ \left(\frac{r_p}{r_p+\Delta}\right)\right]} \quad . \tag{17B}$$

In order to use the above expression, values for T_0 are required. Information concerning T_0 can be obtained by making an energy balance on the droplet surface.

The energy balance developed below follows closely that given by Wright (ref. 28). Assuming the concentration of the surrounding gas to be much greater than the evaporating vapor, the heat transferred to the drop will be mainly due to the gas. Molecules emerging from the gas at a distance Δ_T from the drop are assumed to have a mean energy given by

$$\left(\frac{j+1}{2}\right) k\, T_{\Delta_T} \tag{18B}$$

where k is the Boltzman constant, j is the number of degrees of freedom and T_{Δ_T} is the temperature at $r_p + \Delta_T$. The mean energy transferred by a molecule incident on a liquid drop of temperature T_0 can be expressed in terms of the thermal accommodation coefficient α_T for translational energy; there results

$$\alpha_T \left[T_{\Delta_T} - T_0\right] \left(\frac{j+1}{2}\right) k \ . \tag{19B}$$

To obtain the total energy transferred, the above energy per molecule is multiplied by the rate at which molecules strike the surface so that the rate of supply of heat can be written as

$$\dot{Q} = 4\pi r_p^{\,2} \alpha_T \nu_{\Delta_T} \left(\frac{p_{\Delta_T}}{T_{\Delta_T}}\right) \left(\frac{j+1}{2}\right) \left(T_{\Delta_T} - T_0\right) \ . \tag{20B}$$

Since the heat transfer rate by conduction at $r_p + \Delta_T$ is given by

$$\dot{Q} = 4\pi(r_p + \Delta_T)\, \lambda\, (T_\infty - T_{\Delta_T}) \tag{21B}$$

and since the rates expressed by (20B) and (21B) are equal, one can solve for

$$T_{\Delta_T} - T_0 = \frac{\lambda(r_p + \Delta_T)(T_\infty - T_0)}{\left[\alpha_T r_p^2 \nu_{\Delta_T} \frac{p_{\Delta_T}}{T_{\Delta_T}} \left(\frac{j+1}{2}\right) + \lambda(r_p + \Delta_T)\right]} \quad . \tag{22B}$$

Under conditions of steady evaporation

$$\dot{Q} = \dot{m}L \tag{23B}$$

which can be combined with (20B) and (22B) resulting in

$$\dot{m}L = \frac{4\pi r_p \lambda (T_\infty - T_0)}{2\lambda T_{\Delta_T} \left\{ \left[\frac{}{\alpha_T \nu_{\Delta_T} r_p (j+1)}\right] + \left(\frac{r_p}{r_p + \Delta_T}\right)\right\}} \quad . \tag{24B}$$

From Wright (ref. 21), we take

$$\Delta_T = \frac{\lambda T_{\Delta_T}}{\nu_{\Delta_T} p_{\Delta_T} \left(\frac{j+1}{2}\right)} \quad . \tag{25B}$$

Thus,

$$\dot{m}L = \frac{4\pi r_p \lambda (T_\infty - T_0)}{\left[\frac{2}{\alpha_T} \frac{\Delta_T}{r_p} + \frac{r_p}{r_p + \Delta_T}\right]} \quad . \tag{26B}$$

Equations (17B) and (26B) can be used to express the concentration at the drop surface as

$$c_o = \frac{\lambda(T_\infty - T_0)}{DL\left[1 - \sqrt{\frac{T_\Delta}{T}} \frac{\bar{M}_\infty \bar{c}_\Delta}{\bar{M}_\Delta \bar{c}_\infty}\right) \frac{c_\infty}{c_o}]} \frac{\left[\frac{2}{\alpha} \frac{\Delta}{r_p} + \sqrt{\frac{T_\Delta}{T_0}} \left(\frac{r_p}{r_p + \Delta}\right)\right]}{\left[\frac{2}{\alpha_T} \frac{\Delta_T}{r_p} + \left(\frac{r_p}{r_p + \Delta_T}\right)\right]} \quad . \tag{27B}$$

Taking $c_o = \frac{p_o M_p}{R_0 T_0}$, we have

$$p_o = \frac{\lambda R_0 T_0}{M_p DL} \frac{T_\infty - T_0)}{[1 - (\sqrt{\frac{T_\Delta}{T_0}} \frac{\bar{M}_\infty \bar{c}_\Delta}{\bar{M}_\Delta \bar{c}_\infty}) \frac{c_\infty}{c_o}]} \frac{[\frac{2}{\alpha} \frac{\Delta}{r_p} + \sqrt{\frac{T_\Delta}{T_0}} (\frac{r_p}{r_p + \Delta})]}{[\frac{2}{\alpha_T} \frac{\Delta_T}{r_p} + (\frac{r_p}{r_p + \Delta_T})]} . \quad (28B)$$

Since $p_o = f(T_0)$ the above expression can be used to solve for the droplet temperature provided all terms on the right hand side are known. Values of the properties at $r_p + \Delta$ and $r_p + \Delta_T$ are unknown. For simplicity, the values at $r_p + \Delta$ are taken as those corresponding to the droplet surface, and the values at $r_p + \Delta_T$ those of the gas at large distance from the drop. In addition, we take $c_\infty = 0$ since the spray is considered dilute and the heat balance was made for evaporation into a large excess of gas. Using these assumptions, the final expressions for the evaporation rate and the saturation pressure at the droplet temperature become

$$\dot{m} = \frac{4\pi r_p D p_o M_p}{R_0 T_0 [\frac{2}{\alpha} \frac{\Delta}{r_p} + \frac{r_p}{r_p + \Delta}]} \quad (29B)$$

and

$$p_o = \frac{\lambda R_0 T_0 (T_\infty - T_0)}{M_p DL} \frac{[\frac{2}{\alpha} \frac{\Delta}{r_p} + \frac{r_p}{r_p + \Delta}]}{[\frac{2}{\alpha_T} \frac{\Delta_T}{r_p} + \frac{r_p}{r_p + \Delta_T}]} . \quad (30B)$$

Combining equations (29B) and (30B) and normalizing the result according to the definitions given in Appendix E, the following dimensionless expression for $R' \equiv \frac{dr_p}{dt} = - \frac{\dot{m}}{4\pi m_p r_p^2}$ is obtained:

$$R' = - \frac{\chi}{r_p} \quad (31B)$$

where

$$\chi = \frac{p_o D}{T_0} [\frac{2}{\alpha} \frac{\Delta}{r_p} + \frac{r_p}{r_p + \Delta}]^{-1} . \quad (32B)$$

The dimensionless form of (30B) is

$$p_o = \frac{\lambda T_o}{LD} \left(T_\infty - \beta_7 T_o\right) \frac{\left[\frac{2}{\alpha}\frac{\Delta}{r_p} + \frac{r_p}{r_p+\Delta}\right]}{\left[\frac{2}{\alpha_T}\frac{\Delta_T}{r_p} + \frac{r_p}{r_p+\Delta_T}\right]} \quad . \tag{33B}$$

In this work, it is assumed that $\alpha_T = 1$ and $\alpha = .05$ which approximates the value $\alpha = .034$ given by Fuchs (ref. 22) for pure water.

APPENDIX C
SPRAY DRAG

Forces Acting on the Spray

The equations derived in Appendix A are expressed in terms of a quantity $\vec{F}$ representing the force per unit mass exerted on a drop by the surrounding gas. Contributions to $\vec{F}$ may include (ref. 9): (a) skin friction and separation drag, (b) body forces such as gravity, (c) droplet rotation, (d) pressure gradients in the gas. However, effect (a) is usually largest for sprays and will be the only effect considered in this work.

In terms of a drag coefficient C_D, the expression for $\vec{F}$ for a spherical drop of radius r_p may be expressed as

$$\vec{F} = \frac{3\rho_g C_D}{8 m_p r_p} (\vec{V}_g - \vec{V}_p) |\vec{V}_g - \vec{V}_p| \tag{1C}$$

thus, (1C) becomes, in dimensionless form

$$\vec{\bar{F}} = \frac{3\rho_g C_D}{8 r_p} (\vec{V}_g - \beta_2 \vec{V}_p) |\vec{V}_g - \beta_2 \vec{V}_p| \ . \tag{2C}$$

Droplet Drag Coefficient

Sphere drag coefficients as a function of Reynolds number are usually taken from the so-called "standard drag curve," which is applicable to the uniform motion of a single solid sphere in an infinitely extended, still, isothermal, incompressible fluid. However, the environment of the spray is quite different from the conditions upon which the standard drag curve is based. The spray is being accelerated by a medium which is itself accelerating, giving rise to unsteady drag. Increased turbulence intensity due to the disturbing effect of the droplets, droplet rotation and changes in the variation of the gas viscosity near the drops because of the heat and mass transfers can also affect the drag. Rarefaction effects must also be considered.

As shown in Appendix B, the drops are expected to be in either the transition or free-molecule regime. Figure 13 represents a plot of sphere drag coefficient data for both transition and continuum supersonic flows, (refs. 32-36). The solid line is the curve fit

$$C_D = 2(Re/M)^{-.0867} \ , \quad 1 < \frac{Re}{M} < 10^4 \ . \tag{3C}$$

This coarse approximation is more than satisfactory in view of the fact that the conditions under which the data were obtained were not typical of the

actual environment of the spray drops. In the free molecule regime, the drag coefficient is taken as that for diffuse reflection (ref. 19)

$$C_D = \frac{e^{-S^2/2}}{\pi S^3}\left(1 + 2S^2\right) + \frac{4S^4 + 4S^2 - 1}{2S^4}\,\mathrm{erf}(S) + \frac{2\sqrt{\pi}}{3S_w} \tag{4C}$$

where $S = \dfrac{|\vec{V}_g - \vec{V}_p|}{\sqrt{\dfrac{2R_0T_g}{M_g}}}$ and $S_w = \dfrac{|\vec{V}_g - \vec{V}_p|}{\sqrt{\dfrac{2R_0T_p}{M_g}}}$ (5C)

are the speed ratios for the undisturbed gas and for reflected air molecules at the drop temperature, respectively. Here erf(s) is the error function.

APPENDIX D
THERMODYNAMIC AND TRANSPORT PROPERTIES

Introduction

The gaseous medium acting upon the spray is a mixture of ionized air and water vapor. However, the water vapor content of the mixture relative to the air is assumed small enough so that its effect may be neglected when calculating the thermodynamic and transport properties of the gas. In addition, the ionic species of the air are neglected when making these calculations. Hence, the thermodynamic and transport property values are desired for a high temperature dissociated air mixture consisting of the five species N_2, O_2, N_O, N and O.

Thermodynamic Properties

Gas Specific Heat and Enthalpy. Using the usual mixture rules, the frozen specific heat at constant pressure is

$$C_{pg} = \sum_{i=1}^{N} X_i C_{pgi} , \quad i = 1,2,\ldots,N \tag{1D}$$

and for the mixture molar enthalpy

$$h_g = \sum_{i=1}^{N} X_i h_{gi}, \quad i = 1,2,\ldots,N \tag{2D}$$

where X_i are the species mole fractions and N is the total number of species. Values for the specific heats and enthalpies of the various species were obtained from a least-squares curve fit of the data given by Wilkins (ref. 37). The curve fit was made over the range ($200^oK < T_g < 6000^oK$). At temperatures above 6000^oK the specific heats were taken as constant at their value at 6000^oK, and the enthalpies were calculated from the resulting linear expressions. Values for the heats of formation were taken from Wilkins.

Droplet Enthalpy. For the droplet enthalpy, we have

$$h_p = \int_{T_O}^{T_p} C_s dT + h_{pf_o} \tag{3D}$$

where C_s is the liquid specific heat, T_p the droplet temperature, T_O a reference temperature and h_{pf_o} the droplet heat of formation at the temperature T_O.

Assuming C_S to be constant and taking $T_o = 0^oK$, there results

$$h_p = C_S T_p + h_{pf_o} \quad . \tag{4D}$$

Droplet Latent Heat of Vaporization. The temperature dependence of the latent heat of vaporization of the liquid drops, L, was obtained by a linear curve fit of the data given by Smithsonian Meterological Tables (ref. 25).

Transport Properties

Assumptions. Calculations for the transport properties are very complicated for mixtures with as many as five components. According to Yun and Mason (ref. 38) transport properties of dissociated air calculated using the "atom-molecule" binary approximation are unlikely to be in error by as much as 5 percent when using the correct species concentration. Since more accurate transport calculations are not required in this work, this so-called binary model for the air mixture will be used. In this approximation, N_2, O_2 and NO are lumped together as molecules, and O and N as atoms. The necessary collision integrals are obtained by considering only three interactions, atom-atom, atom-molecule and molecule-molecule, which are taken to be the same as the corresponding nitrogen interactions.

Transport properties desired are the viscosity, thermal conductivity and the diffusion coefficient. Expressions for the mixture viscosity and thermal conductivity are taken from Brokaw (ref. 39). They represent approximations to the more complex expressions based on rigorous kinetic theory. The diffusion coefficient is calculated using Le = 1.

Viscosity. For a gas mixture of N components, the viscosity is approximated by

$$\mu_{mix} = \sum_{i=1}^{N} \frac{\mu_i}{1 + \sum_{\substack{j=1 \\ j \neq i}}^{N} \phi_{ij} \frac{X_j}{X_i}} \tag{5D}$$

where μ_i are the viscosities of the component gases and X_i is the mole fraction for species i. For the coefficients ϕ_{ij}, we have

$$\phi_{ij} = \frac{\left[1 + \left(\frac{\mu_i}{\mu_j}\right)^{1/2} \left(\frac{M_j}{M_i}\right)^{1/4}\right]^2}{2\sqrt{2}\left(1 + \frac{M_i}{M_j}\right)^{1/2}} \tag{6D}$$

where M_i is the molecular weight of species i. The viscosities of the pure component gases are given by

$$\mu_i = 26.693 \cdot 10^{-6} \frac{\sqrt{M_i T_g}}{\langle \bar{\Omega}_i^{(2,2)} \rangle} \tag{7D}$$

where μ_i has units of (g/cm sec) and the $\langle \bar{\Omega}_i^{(2,2)} \rangle$ represent collision integrals such as those tabulated by Yun and Mason.

Thermal Conductivity. The thermal conductivity of a mixture of polyatomic gases may be written as

$$\lambda_{mix} = \lambda'_{mix} + \lambda''_{mix} \tag{8D}$$

where λ'_{mix} is the monatomic thermal conductivity of the mixture and λ''_{mix} is the mixture contribution to the thermal conductivity by diffusional transport of internal energy.

The monatomic mixture conductivity can be approximated by

$$\lambda'_{mix} = \sum_{i=1}^{N} \frac{\lambda'_i}{1 + \sum_{\substack{j=1 \\ j \neq i}}^{N} \psi_{ij} \frac{X_j}{X_i}} \tag{9D}$$

where the λ'_i are the monatomic thermal conductivities of the pure component gases, given by

$$\lambda'_i = \frac{15 R_0}{4 M_i} \mu_i \, . \tag{10D}$$

For the ψ_{ij}, we have

$$\psi_{ij} = \phi_{ij} \left[1 + 2.41 \frac{(M_i - M_j)(M_i - .142 M_j)}{(M_i + M_j)^2} \right] \tag{11D}$$

and the ϕ_{ij} are as previously given by (6D). The expression used for λ''_{mix} is

$$\lambda''_{mix} = \sum_{i=1}^{N} \frac{\lambda''_i}{1 + \sum_{\substack{i=1 \\ j\neq 1}}^{N} \phi_{ij} \frac{X_j}{X_i}} \qquad (12D)$$

where the λ''_i are the internal thermal conductivities of the pure component gases, given approximately by

$$\lambda''_i = .88 \left(\frac{2C_{pgi}}{5R_0} - 1\right) \lambda'_i \quad . \qquad (13D)$$

Diffusion Coefficient. The Lewis number is defined as

$$Le = \lambda_g / \rho_g D C_{pg} \quad .$$

Taking Le = 1, the diffusion coefficient can be calculated using the previously given results for C_{pg} and λ_g .

APPENDIX E
SYMBOLS

Symbols

C_D	drag coefficient
C_p	specific heat at constant pressure
C_s	liquid specific heat
c	vapor density
D	diffusion coefficient
D_N	vehicle nose diameter
d	droplet diameter
F	drag force per unit mass
f	flux distribution function or spray distribution function
G	flux term
g	size distribution function
H	total enthalpy of gas
h_{pf_o}	heat of formation of liquid
I	flux term
K	source term
k	Boltzman constant
L	heat of vaporization
Le	Lewis number
ℓ	mean free path
M	molecular weight or Mach number
m_p	material density of liquid
$\dot{m}$	evaporation rate or injected liquid mass flow rate
N	atomic nitrogen
N_2	diatomic nitrogen
NO	nitrogen oxide
n	coordinate normal to body
O	atomic oxygen
O_2	diatomic oxygen
p	pressure
p_o	saturation vapor pressure

Q	spray nucleation and breakup
$\dot{Q}$	heat transfer rate
q	integral of flux distribution
R	body radius of curvature
Re	Reynolds number
R'	time rate of change of droplet radius
r	radius of axisymmetric body or radial coordinate
r_p	droplet radius
S	speed ratio
s	coordinate along body
T	temperature
t	time
u	component of gas velocity
V	velocity
v	component of spray velocity
We	Weber number
w	n/ϵ
X	mole fraction
x,y	cartesian coordinates
Z_c	compressibility factor, M_{g_∞}/M_g
z	n/δ
α	evaporation coefficient
α_T	thermal accommodation coefficient
β	dimensionless parameter
Γ	drop collisions
γ	ratio of specific heats
Δ	concentration jump distance or injection length
Δ_T	temperature jump distance
δ	shock layer thickness
δ_D	Dirac delta function
ϵ	penetration distance
θ	local body angle
λ_g	gas thermal conductivity

μ_g	gas viscosity
ν	shock angle
ξ	dependent variable of integral method differential equations
ρ	density
σ_p	droplet surface tension
ϕ	injection angle
χ	evaporation factor
Ω	collision integral

Subscripts

g	gas
I	injection
inj	spray injection value
N	no injection
n	velocity component normal to body
p	spray
s	velocity component along body
δ	shock
ϵ	interface
o	body
oo	free stream

Superscripts

—	dimensional quantity or average value
'	denotes derivative

Normalizing Factors

Except for the quantities listed below, all gas properties were normalized using their corresponding free stream values and all spray properties were normalized using their corresponding initial injection values. The coordinates and geometrical quantities were normalized using the body nose diameter, D_N.

The following normalizing factors were used:

Variable	Normalizing Factor
C_p	$5R_0/2$
D	$\mu_{g_\infty}/\rho_{g_\infty}$
F	$\rho_{g_\infty} V^2_{g_\infty}/m_p r_{p\text{-inj}}$
L	$15\ R_0 T_{g_\infty}/4M_{g_\infty}$
p_o	$\rho_{g_\infty} R_0 T_{g_\infty}/M_p$
R'	$\mu_{g_\infty}/m_p r_{p\text{-inj}}$
T_p	$T_{p\text{-ref}} = 233^oK$
Δ	$r_{p\text{-inj}}$
Δ_T	$r_{p\text{-inj}}$
λ_g	$15\ R_0 \mu_{g_\infty}/4M_{g_\infty}$

REFERENCES

1. Huber, P. W. and Nelson, C. H.: Plasma Frequency and Radio Attenuation. Proceedings of the NASA-University Conference on the Science and Technology of Space Exploration, Vol. 2, NASA SP-11, 1962, pp. 347-360.

2. Huber, P. W. and Sims, T. E.: Research Approaches to the Problem of Reentry Communications Blackout. Proceedings of the Third Symposium on the Plasma Sheath, Vol. 2, AFCRL-67-0280, 1967, pp. 1-33.

3. Broadwell, J. E.: Analysis of the Fluid Mechanics of Secondary Injection for Thrust Vector Control. AIAA Journal, Vol. 1, 1963, pp. 1067-1075.

4. Sehgal, R. and Wu, J.: Thrust Vector Control by Liquid Injection into Rocket Nozzles. Journal of Spacecraft and Rockets, Vol. 1, 1964, pp. 545-551.

5. Zokoski, E. E. and Spaid, F. W.: Secondary Injection of Gases into a Supersonic Flow. AIAA Journal, Vol. 2, 1964, pp. 1689-1696.

6. Billig, F. S.: Supersonic Combustion of Storable Liquid Fuels in Mach 3.0 to 5.0 Air Streams. Tenth International Symposium on Combustion, The Combustion Institute, Pittsburgh, Pennsylvania, 1965, pp. 1167-1178.

7. Evans, J. S.: Reduction of Free Electron Concentration in a Reentry Plasma by Injection of Liquids. Proceedings of the Third Symposium on the Plasma Sheath, Vol. 3, AFCRL-67-0280, 1967, pp. 343-361.

8. Adelberg, M.: Breakup Rate and Penetration of a Liquid Jet in a Gas Stream. AIAA Journal, Vol. 5, 1967, pp. 1408-1415.

9. Williams, F. A.: Combustion Theory. Addison-Wesley Publishing Co., Inc., Reading, Massachusetts, 1965.

10. Dorodnitsyn, A. A.: A Contribution to the Solution of Mixed Problems of Transonic Aerodynamics. Vol. 2 of Advances in Aeronautical Sciences, Th. von Karman, chief editor, Pergamon Press, New York, 1959, pp. 832-844.

11. Xerikos, J. and Anderson, W. A.: A Critical Study of the Direct Blunt Body Integral Method. Report SM-42603, Douglas Aircraft Co., Inc., Santa Monica, California, 1962.

12. Hayes, W. D. and Probstein, R. F.: Hypersonic Flow Theory. Academic Press, New York, 1959.

13. Xerikos, J. and Anderson, W. A.: An Experimental Investigation of the Shock Layer Surrounding a Sphere in Supersonic Flow. AIAA Journal, Vol. 3, 1965, pp. 451-457.

14. Evans, J. S.: Private communication, April, 1967.

15. Volynsky, M. S.: Atomization of a Liquid in a Supersonic Flow. Mekhanika i Mashinostroeniye, Vol. 2, 1963, pp. 20-27.

16. Weaver, W.: Private communication, August, 1967.

17. Lane, W. R.: Shatter of Drops in Streams of Air. Industrial and Engineering Chemistry, Vol. 43, 1951, pp. 1312-1317.

18. Haas, F. C.: Stability of Droplets Suddenly Exposed to a High Velocity Gas Stream. AIChE Journal, Vol. 10, 1964, pp. 920-924.

19. Schaaf, S. A. and Chambre, P. L.: Flow of Rarefied Gases. Fundamentals of Gas Dynamics, sec. H, H. W. Emmons, ed., Princeton University Press, Princeton, New Jersey, 1958, pp. 687-739.

20. Orr, C.: Particulate Technology. The MacMillan Co., New York, 1966.

21. Wright, P. G.: The Effect of the Transport of Heat on the Rate of Evaporation of Small Droplets. Proceedings of the Royal Society of Edinburgh, Series A, Vol. 66, 1962, pp. 65-80.

22. Fuchs, N. A.: Evaporation and Droplet Growth in Gaseous Media. Pergamon Press, New York, 1959.

23. Kennard, E. H.: Kinetic Theory of Gases. McGraw-Hill Book Co., Inc., New York, 1939.

24. Goldsmith, M. and Penner, A. A.: On the Burning of Single Drops of Fuel in an Oxidizing Atmosphere. Jet Propulsion, Vol. 24, 1954, pp. 245-251.

25. Smithsonian Meterological Tables. Sixth Revised Ed., R. J. List, ed., Smithsonian Institution, Washington, D. C., 1951.

26. Langmuir, I.: Dissociation of Hydrogen into Atoms. Journal of the American Chemical Society, Vol. 37, 1915, pp. 417-458.

27. Fuchs, N. A.: On the Theory of the Evaporation of Small Droplets. Soviet Physics--Technical Physics, Vol. 3, 1958, pp. 143-143.

28. Wright, P. G.: On the Discontinuity Involved in Diffusion across an Interface (the Δ of Fuchs). Discussions of the Faraday Society, Vol. 30, 1960, pp. 100-112.

29. Mason, B. J.: Spontaneous Condensation of Water Vapor in Expansion Chamber Experiments. Proceedings of the Physical Society, London, Vol. 64B, 1951, pp. 773-779.

30. Kang, S. W.: Analysis of Condensation Droplet Growth in Rarefied and Continuum Environments. AIAA Journal, Vol. 5, 1967, pp. 1288-1295.

31. Penner, S. S.: Chemistry Problems in Jet Propulsion. Pergamon Press, London, 1957.

32. Aroesty, J.: Sphere Drag in a Low-Density Supersonic Flow. Vol. II of Rarefied Gas Dynamics, J. A. Laurmann, ed., Academic Press, New York, 1963, pp. 261-277.

33. Kinslow, M. and Potter, J. L.: The Drag of Spheres in Rarefied Hypervelocity Flow. Report No. AEDC-TDR-62-205, Arnold Engineering Development Center, Arnold Air Force Station, Tennessee, 1962.

34. Kane, J. J. and Li, F.: Ablation Effects on RF Attenuation in the Turbulent Boundary Layer. AIAA Journal, Vol. 3, 1965, pp. 1558-1559.

35. Masson, D. J., Morris, D. N., and Bloxsom, D. E.: Measurements of Sphere Drag from Hypersonic Continuum to Free-Molecule Flow. Rarefied Gas Dynamics, L. Talbot, ed., Academic Press, New York, 1961, pp. 643-661.

36. May, A. and Witt, W. R., Jr.: Free-flight Determinations of the Drag Coefficients of Spheres. Journal of the Aeronautical Sciences, Vol. 20, 1953, pp. 635-638.

37. Wilkins, R. L.: Theoretical Evaluation of Chemical Propellants. Prentice-Hall, Inc., Englewood Cliffs, New Jersey, 1963.

38. Yun, K. S. and Mason, E. A.: Collision Integrals for the Transport Properties of Dissociating Air at High Temperatures. Physics of Fluids, Vol. 5, 1962, pp. 380-386.

39. Brokaw, R. S.: Alignment Charts for Transport Properties Viscosity, Thermal Conductivity, and Diffusion Coefficients for Nonpolar Gases and Gas Mixtures at Low Density. NASA TR R-81, 1961.

TABLE I

NASA RAM C FLOW PROPERTIES AT INITIAL INJECTION STATION (REF. 14)

n (cm)	T_g (°K)	ρ_g (g/cm^3)	V_g (cm/sec)	X_{N_2}	X_{O_2}	X_N	X_O	X_{NO}
0 body	3342	$1.584 \cdot 10^{-7}$	$4.071 \cdot 10^{5}$	$1.987 \cdot 10^{-1}$	$1.665 \cdot 10^{-7}$	$5.493 \cdot 10^{-1}$	$2.514 \cdot 10^{-1}$	$1.002 \cdot 10^{-4}$
0.946	4177	$1.549 \cdot 10^{-7}$	$4.724 \cdot 10^{5}$	$2.912 \cdot 10^{-1}$	$7.215 \cdot 10^{-6}$	$4.369 \cdot 10^{-1}$	$2.695 \cdot 10^{-1}$	$1.435 \cdot 10^{-3}$
1.998	5794	$1.335 \cdot 10^{-7}$	$5.331 \cdot 10^{5}$	$4.274 \cdot 10^{-1}$	$5.277 \cdot 10^{-4}$	$2.680 \cdot 10^{-1}$	$2.810 \cdot 10^{-1}$	$2.170 \cdot 10^{-2}$
3.189	6524	$1.779 \cdot 10^{-7}$	$5.950 \cdot 10^{5}$	$5.521 \cdot 10^{-1}$	$5.076 \cdot 10^{-3}$	$1.099 \cdot 10^{-1}$	$2.570 \cdot 10^{-1}$	$7.550 \cdot 10^{-2}$
4.835	6418	$4.045 \cdot 10^{-7}$	$6.764 \cdot 10^{5}$	$7.706 \cdot 10^{-1}$	$1.828 \cdot 10^{-1}$	$5.974 \cdot 10^{-4}$	$3.920 \cdot 10^{-2}$	$6.849 \cdot 10^{-3}$
5.343 shock	5200	$6.440 \cdot 10^{-7}$	$7.070 \cdot 10^{5}$	$7.900 \cdot 10^{-1}$	$2.100 \cdot 10^{-1}$	0	0	0

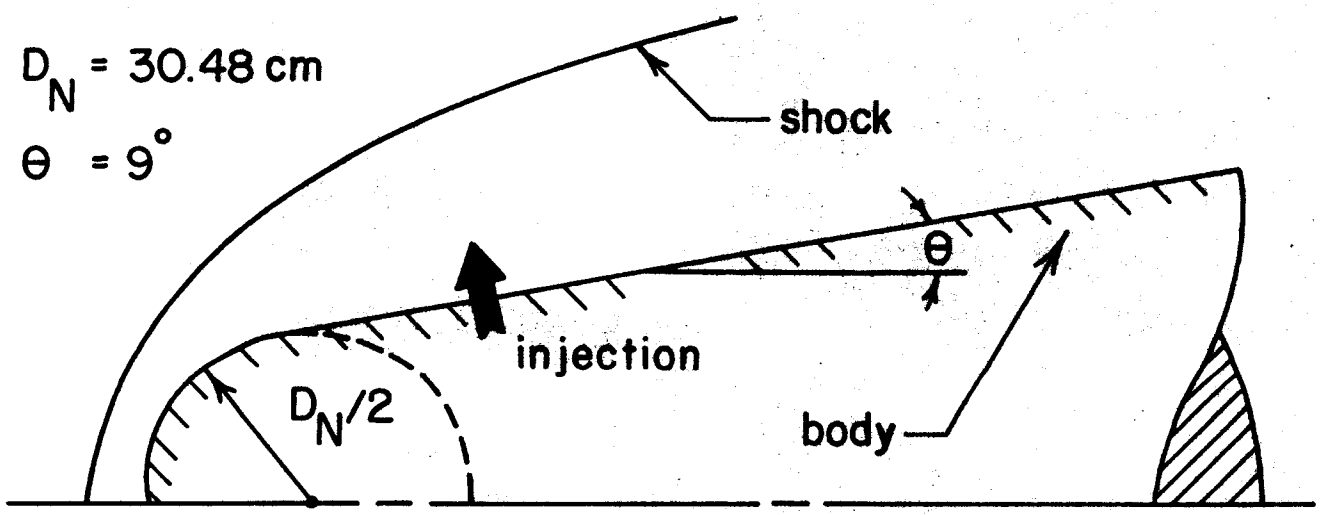

Figure 1. Vehicle geometry

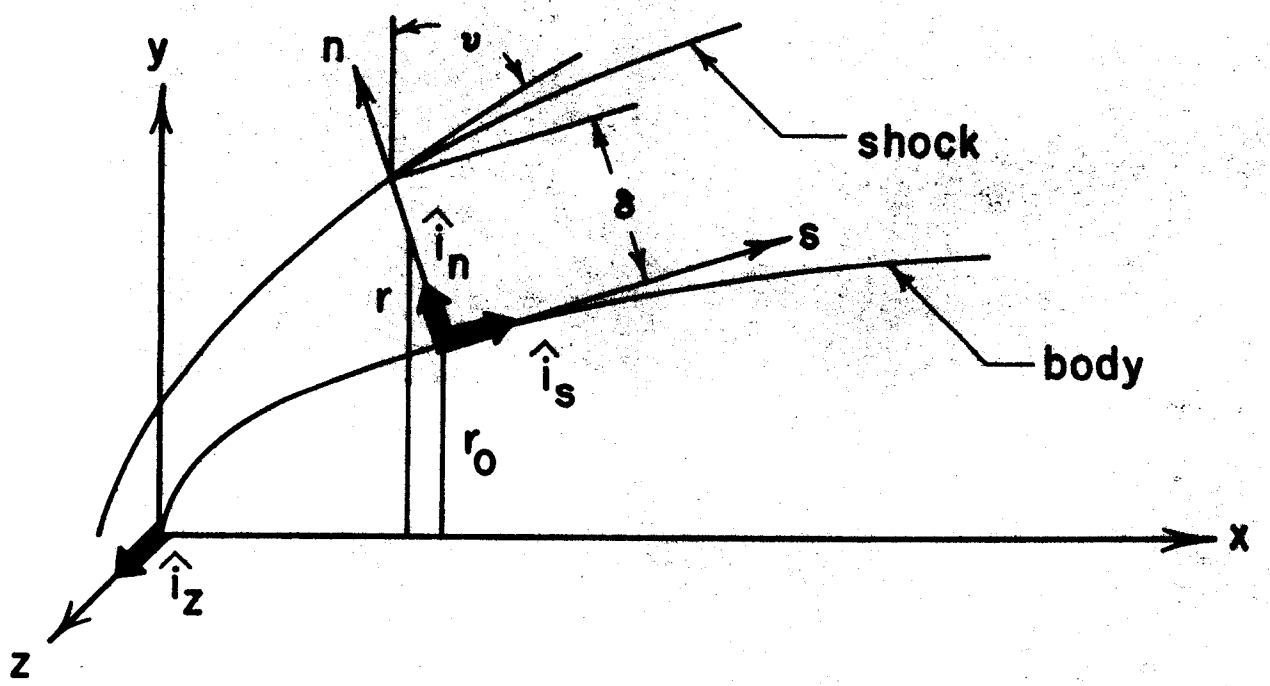

Figure 2. Coordinate system and notation

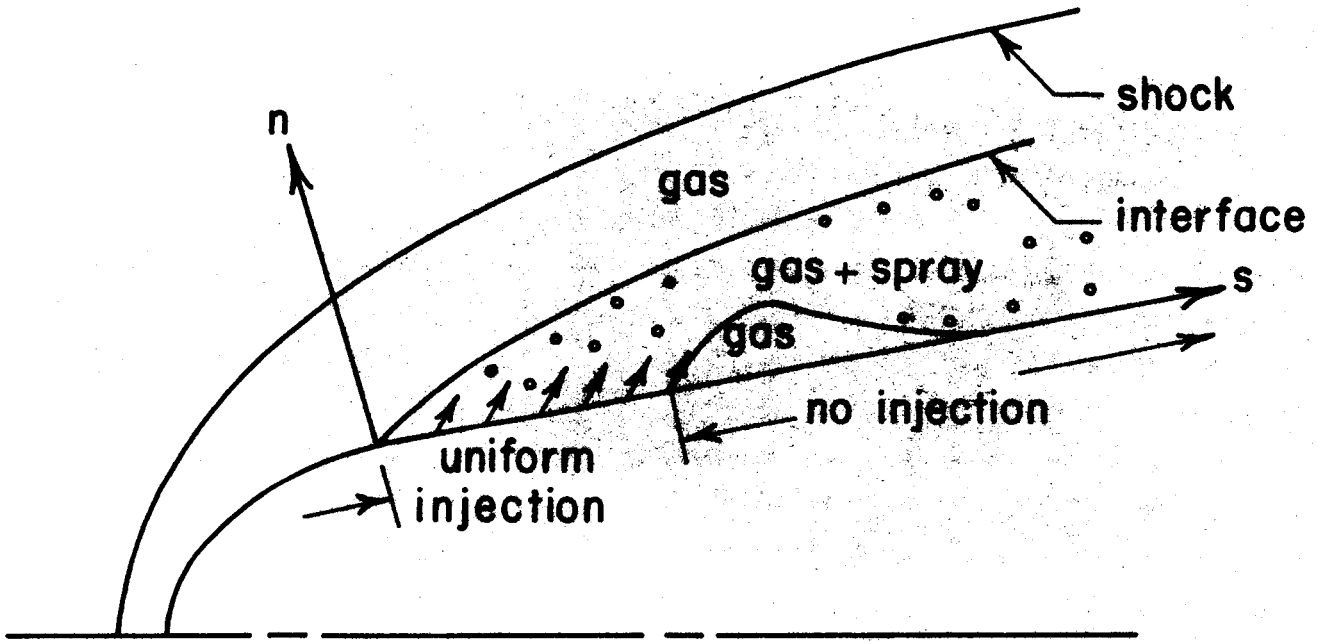

Figure 4. Schematic of gas-spray interaction downstream of injection

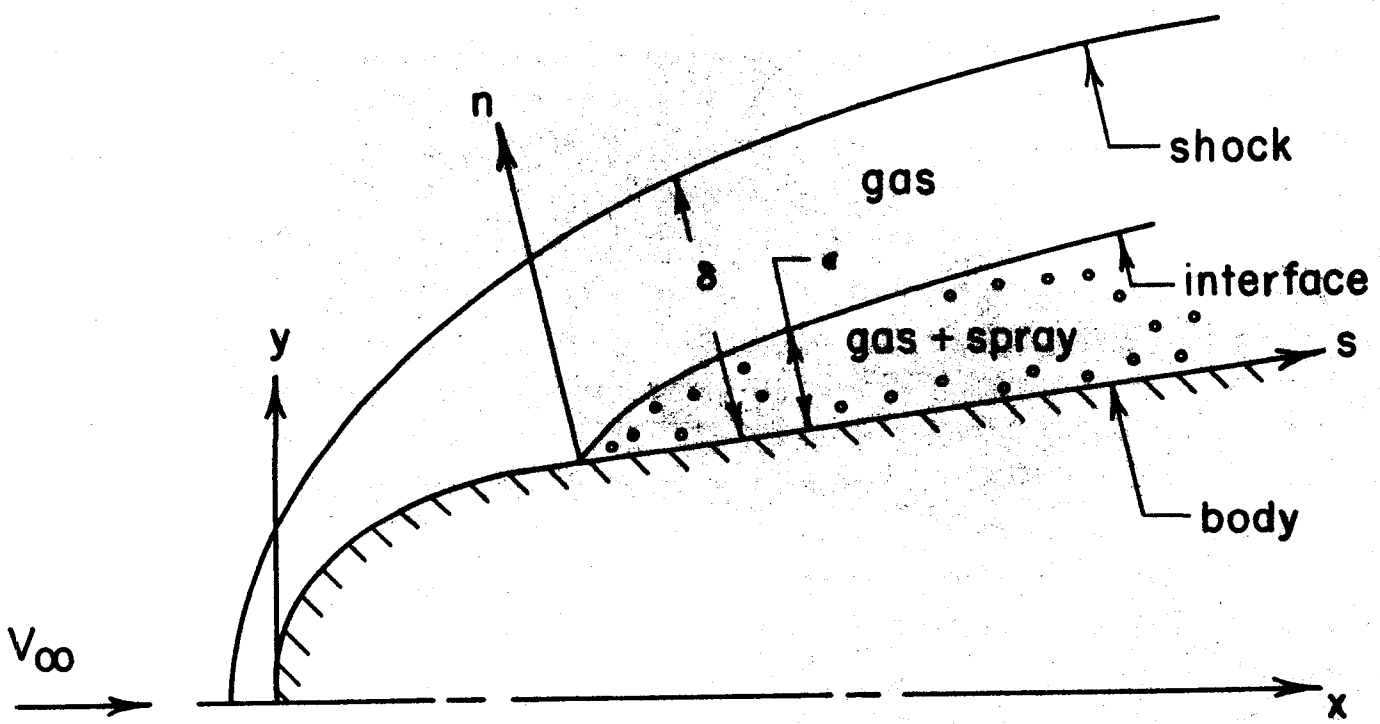

Figure 3. Schematic of the flow field

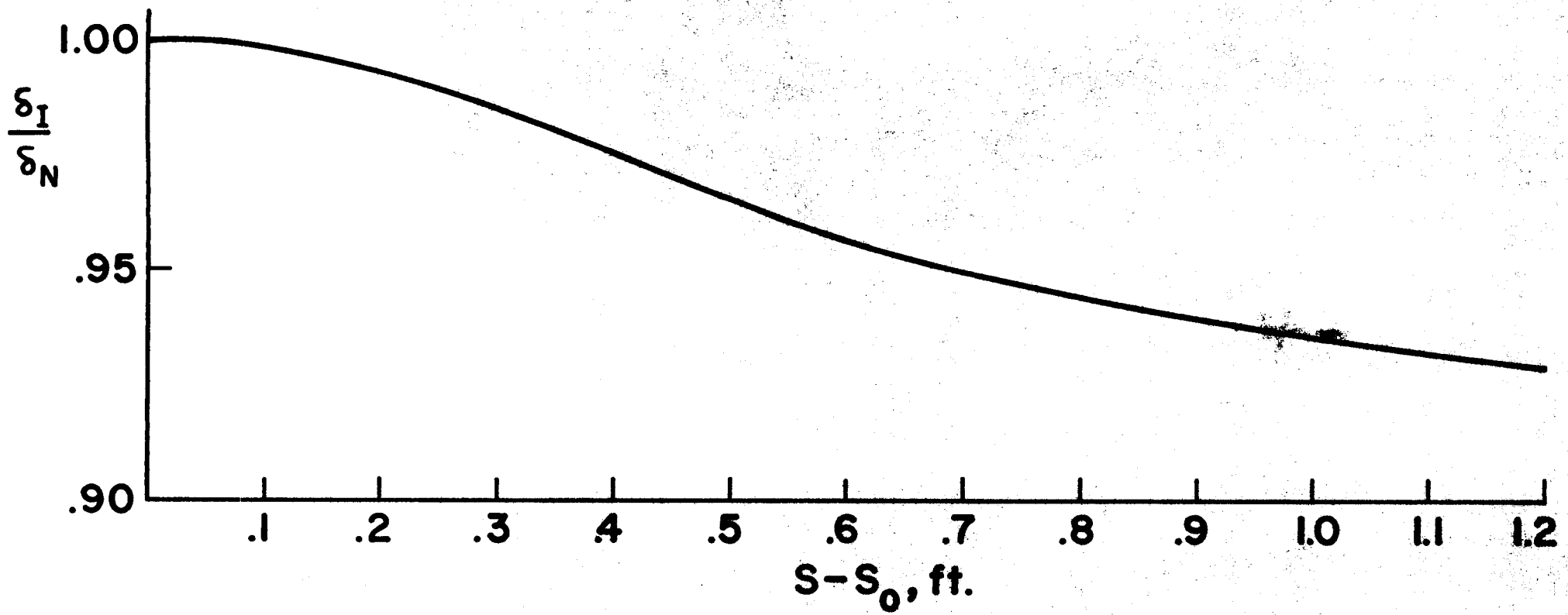

Figure 5. Influence of injection on shock layer thickness.

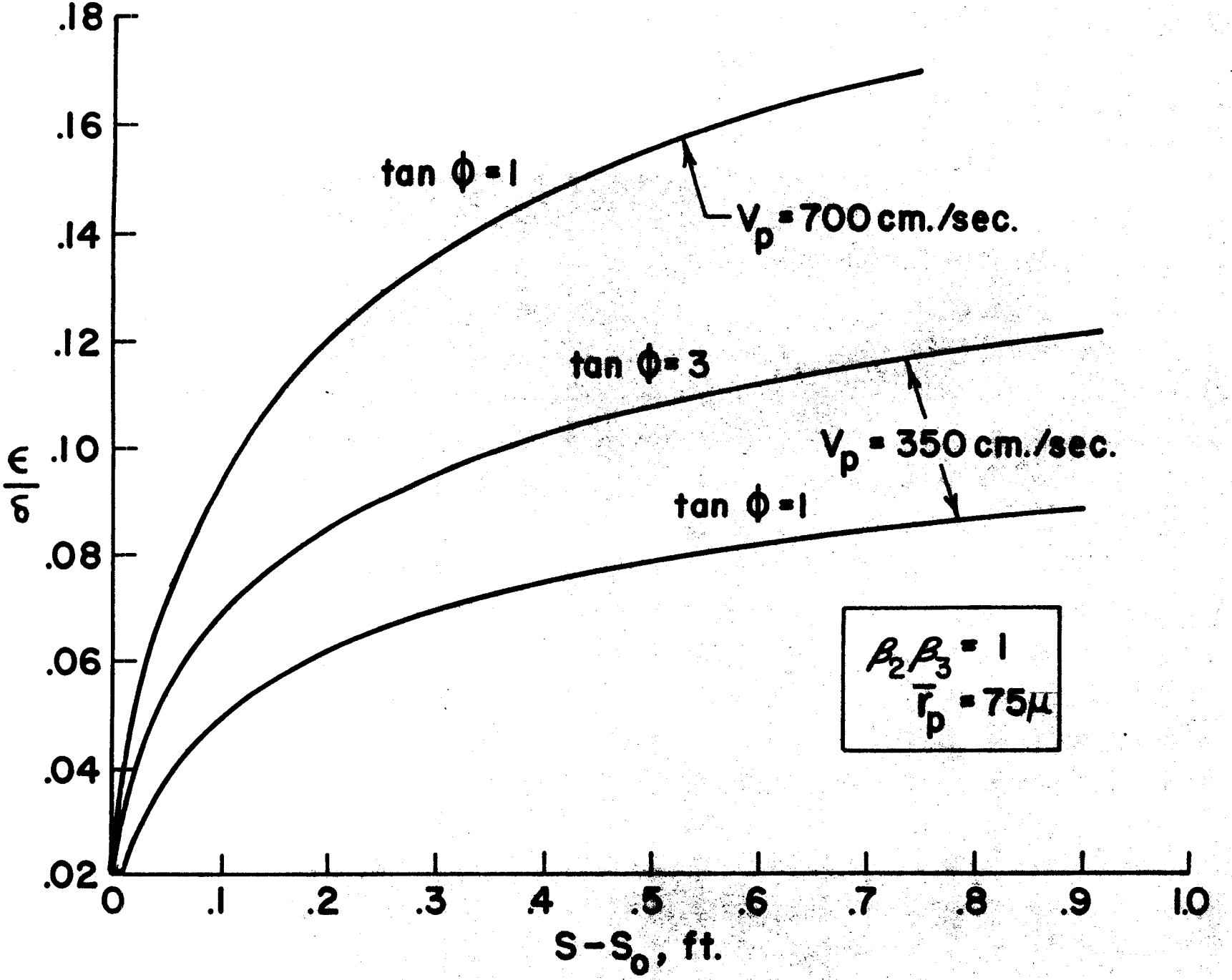

Figure 6. Influence of injection speed and angle on penetration.

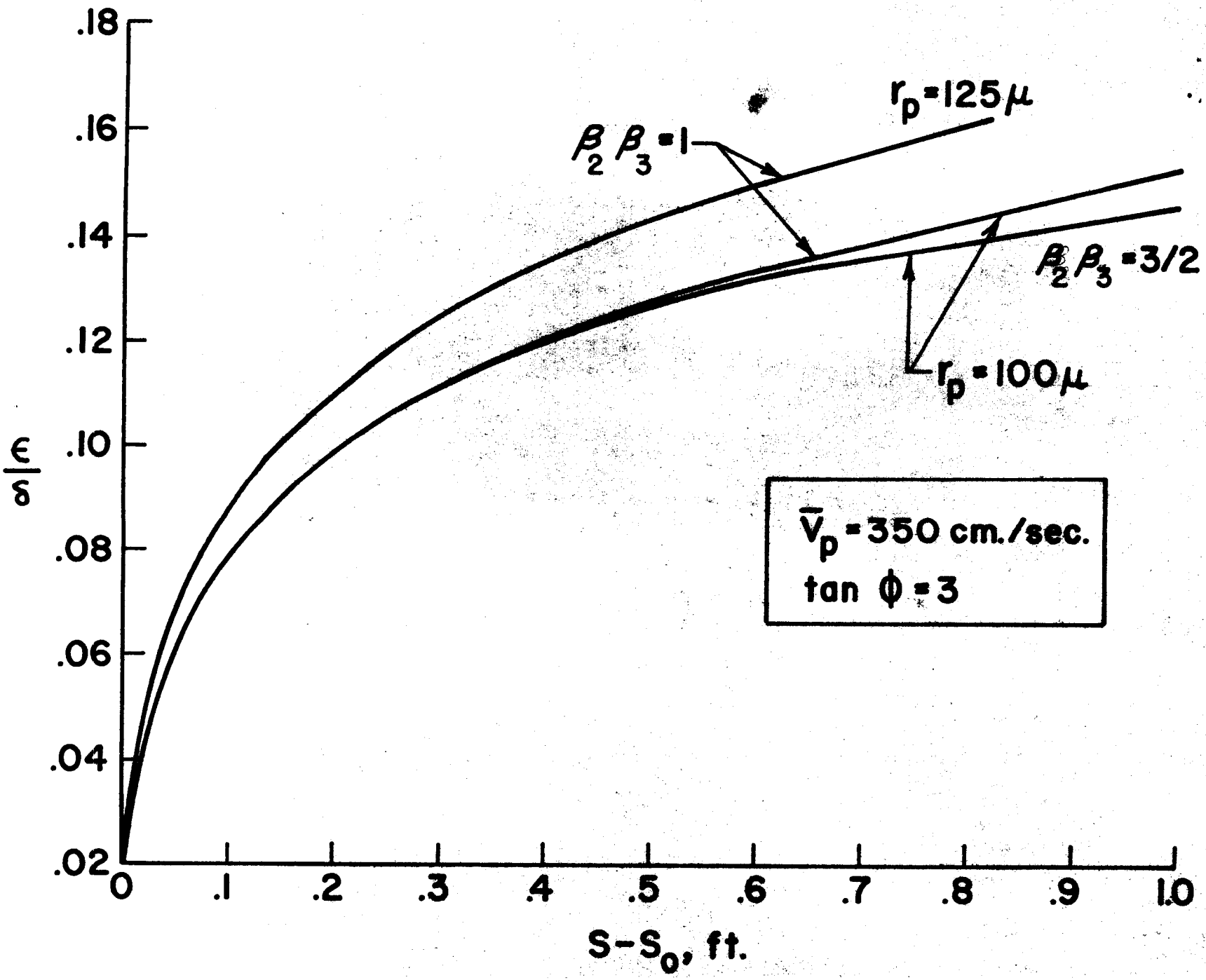

Figure 7. Influence of injection droplet size and mass flow rate on penetration.

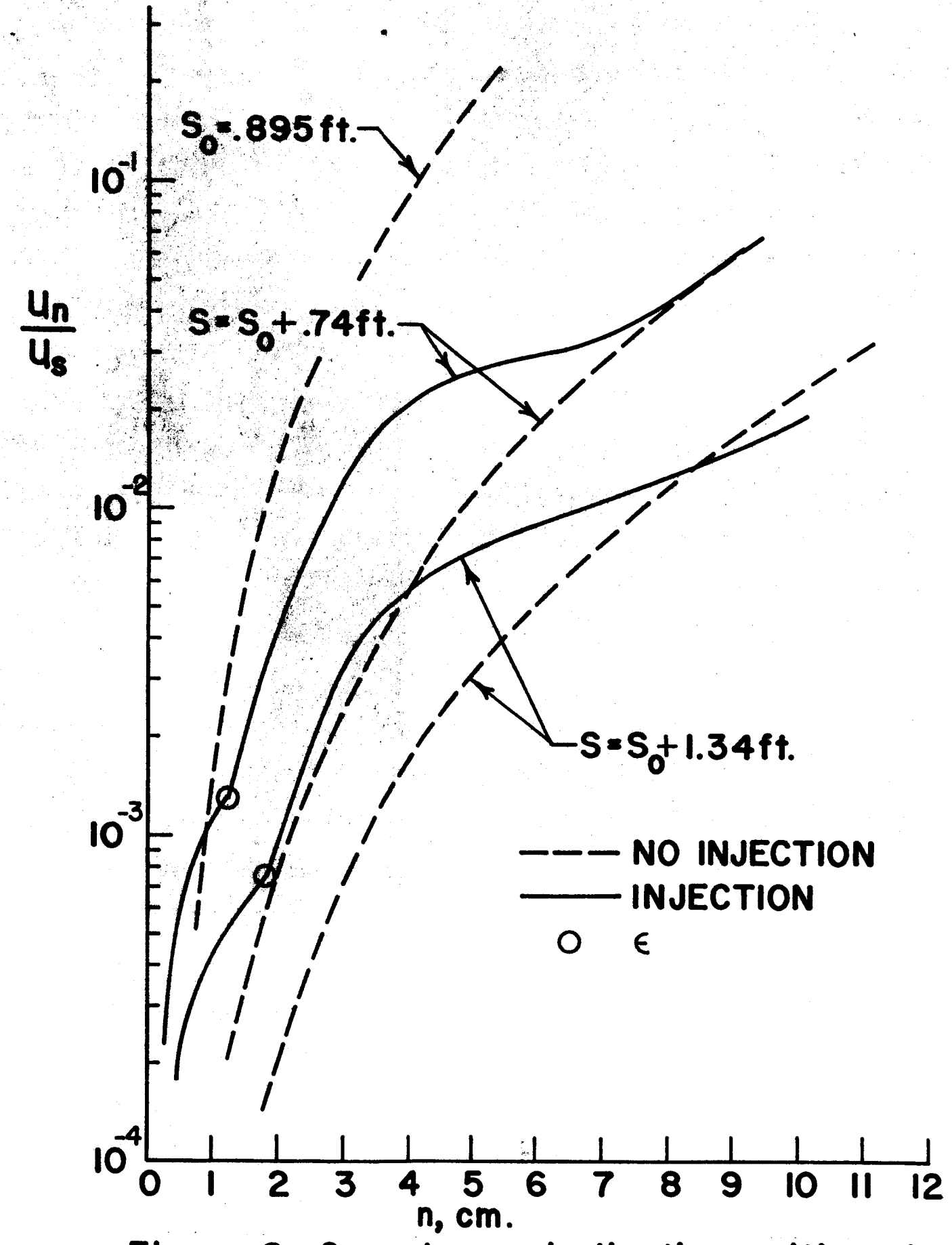

Figure 8. Gas stream inclinations with and without injection.

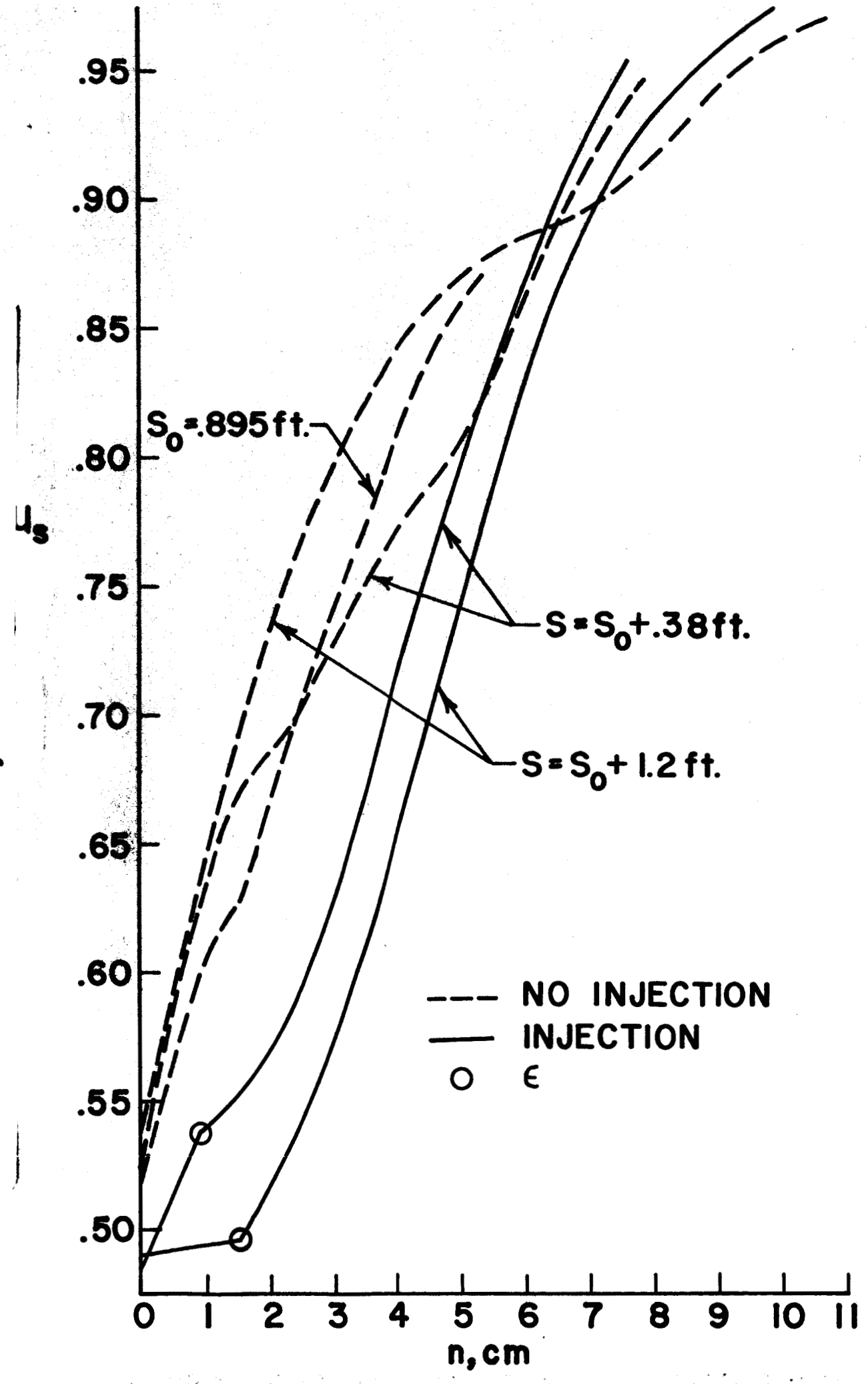

Figure 9. Tangential gas velocity with and without injection.

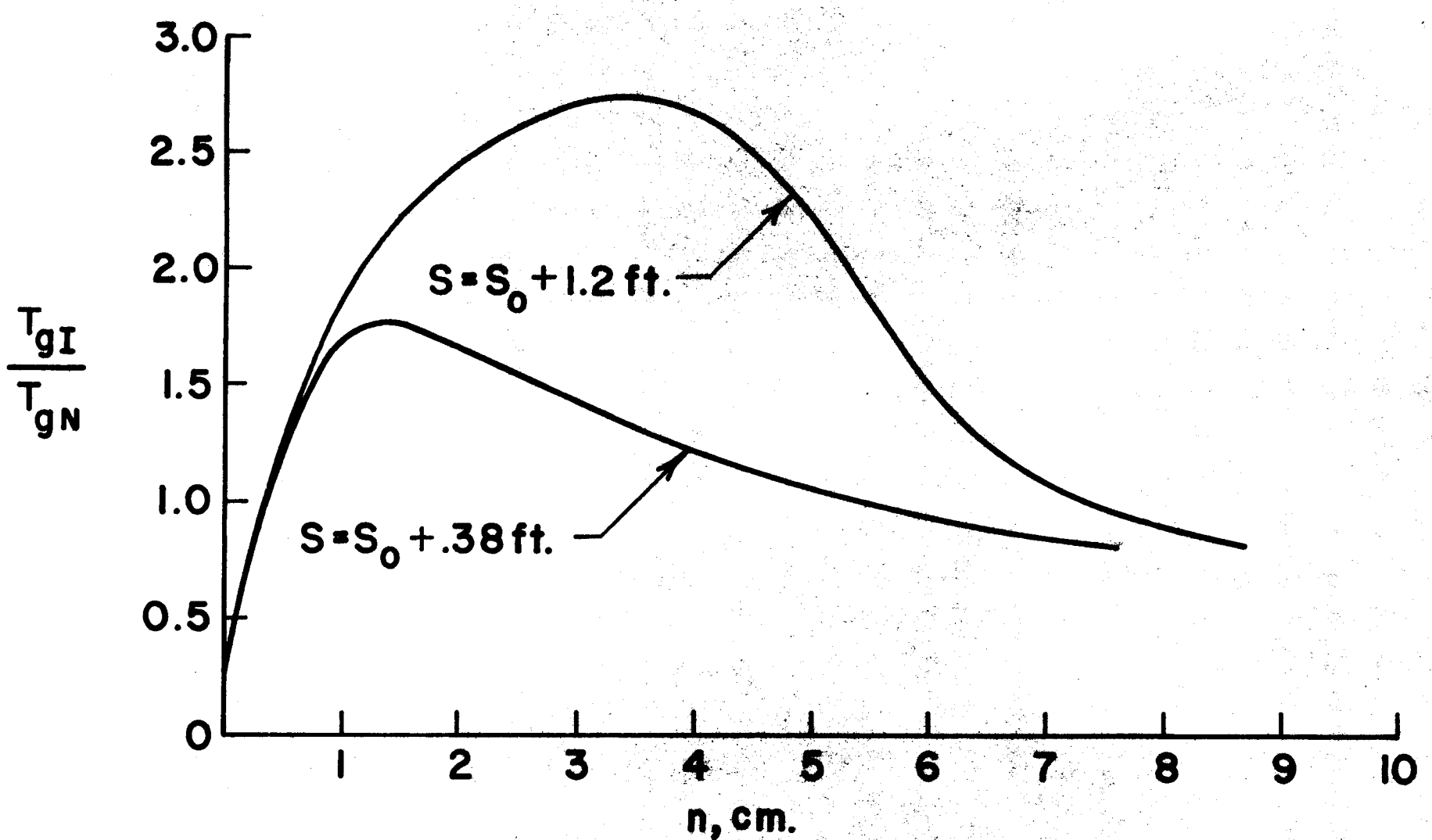

Figure 10. Influence of injection on gas temperature.

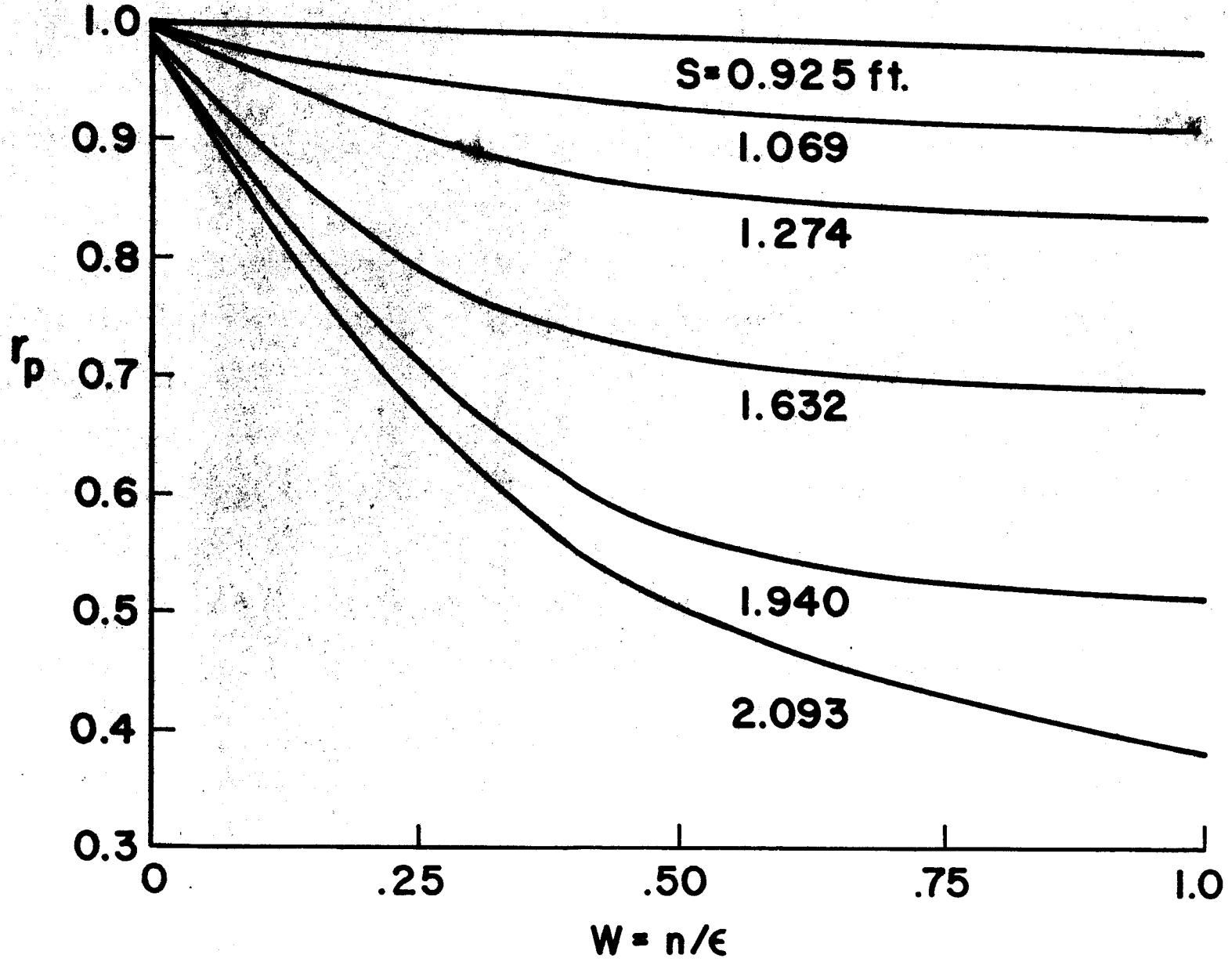

Figure 11. Droplet radius

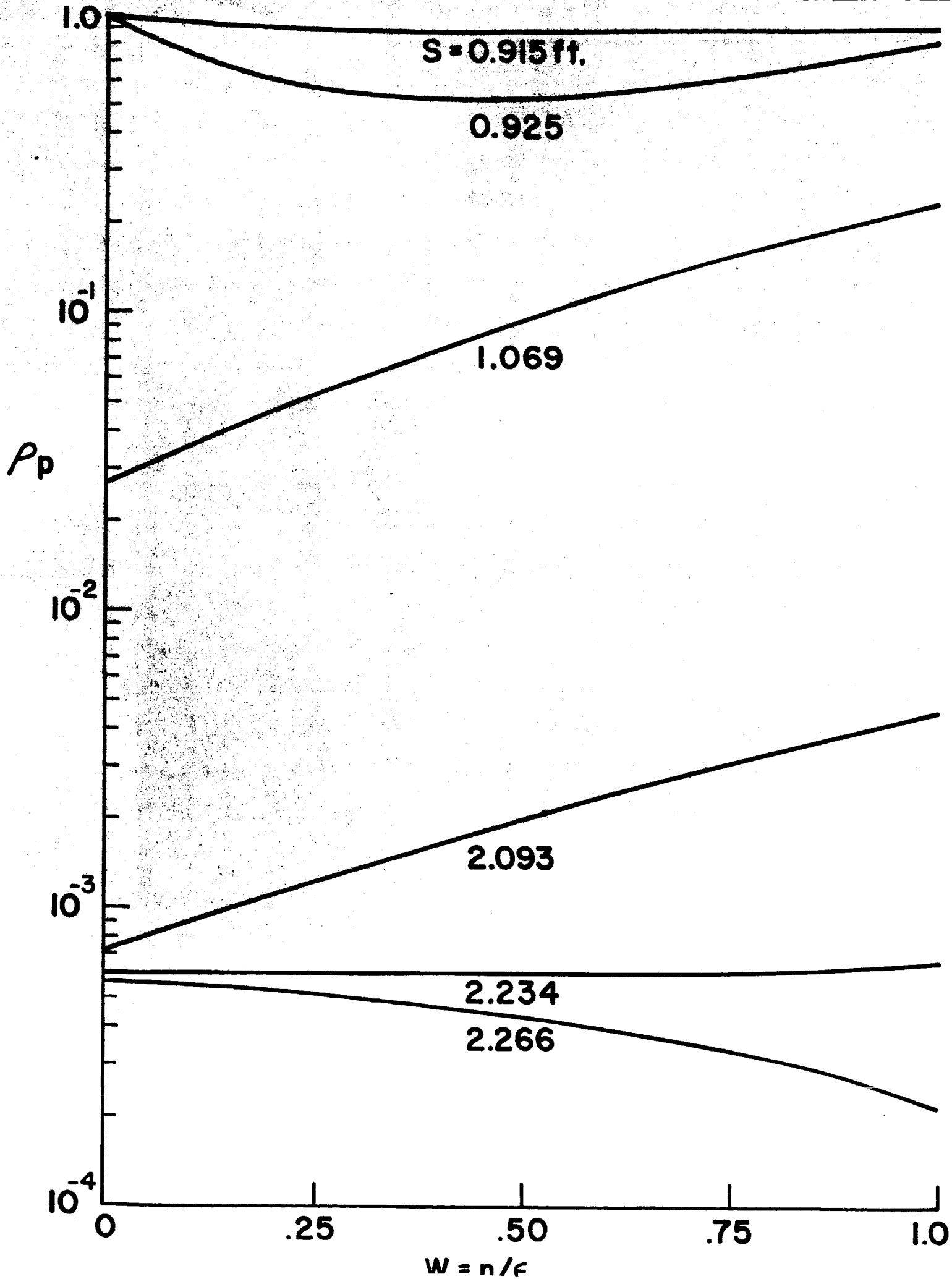

Figure 12. Spray density

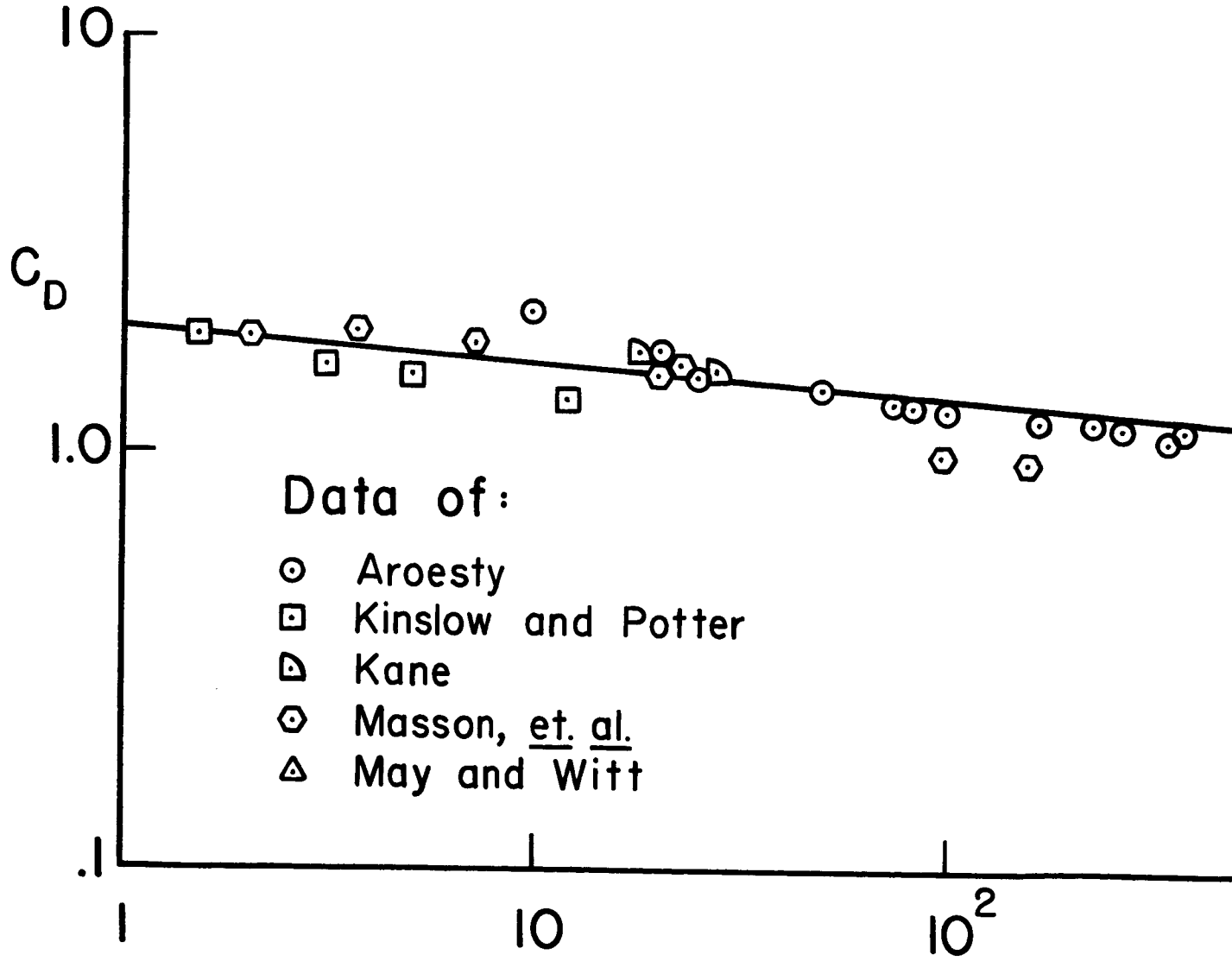

Figure 13. Sphere dr

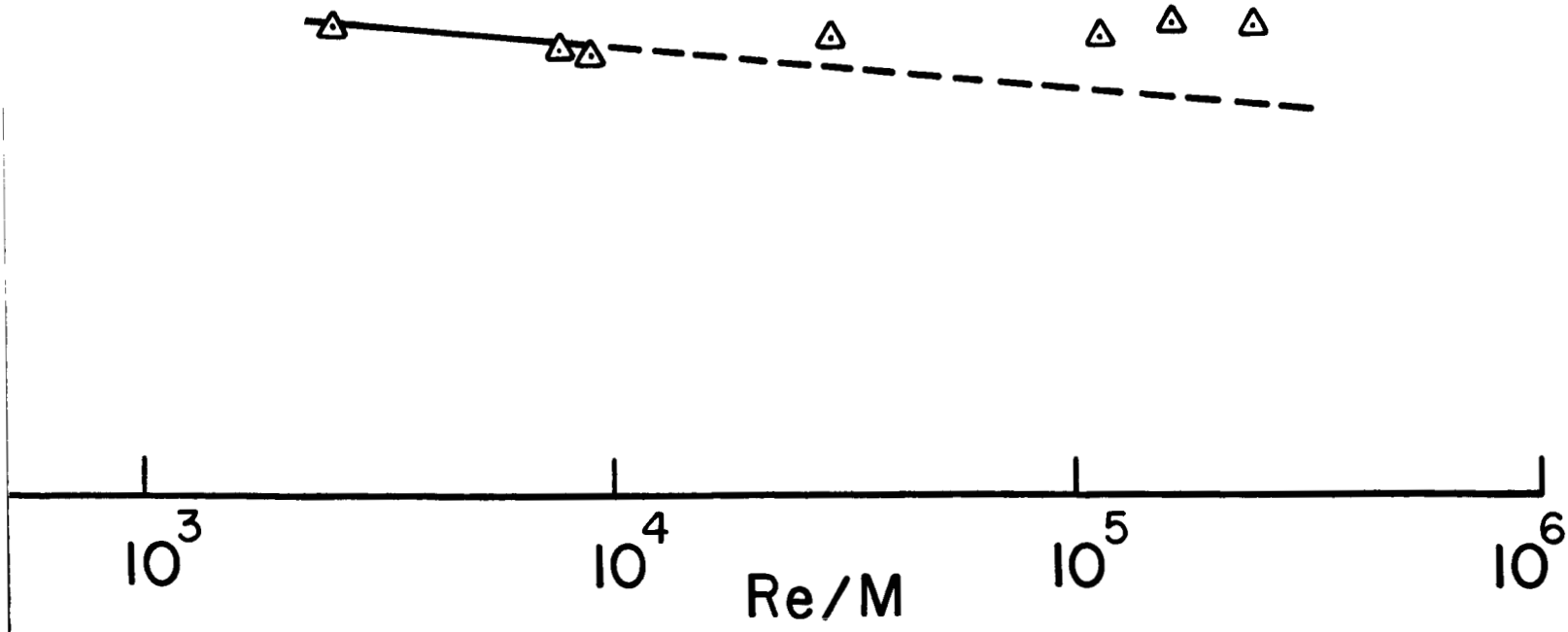

ag coefficient.